Properties and baroclinic instability of stratified thermal upper-ocean flow

F. J. Beron-Vera and

Department of Atmospheric Sciences, Rosenstiel School of Marine, Atmospheric & Earth Science,
University of Miami, Miami, Florida, USA,
e-mail: fberon@miami.edu

M. J. Olascoaga

Department of Ocean Sciences, Rosenstiel School of Marine, Atmospheric & Earth Science,
University of Miami, Miami, Florida, USA,
e-mail: jolascoaga@miami.edu

We study the properties of, and investigate the stability of a baroclinic zonal current in, a thermal rotating shallow-water model, sometimes called *Ripa's model*, featuring stratification for quasigeostrophic upper-ocean dynamics. The model has Lie–Poisson Hamiltonian structure. In addition to Casimirs, the model supports weak Casimirs forming the kernel of the Lie-Poisson bracket for the potential vorticity evolution independent of the details of the buoyancy as this is advected under the flow. The model sustains Rossby waves and a neutral model, whose spurious growth is prevented by a positive-definite integral, quadratic on the deviation from the motionless state. A baroclinic zonal jet with vertical curvature is found to be spectrally stable for specific configurations of the gradients of layer thickness, vertically averaged buoyancy, and buoyancy frequency. Only a subset of such states was found Lyapunov stable using the available integrals, except the weak Casimirs, whose role in constraining stratified thermal flow remains to be understood. The existence of Lyapunov-stable states enabled us to *a priori* bound the nonlinear growth of perturbations to spectrally unstable states. Our results do not support the generality of earlier numerical evidence on the suppression of submesoscale wave activity as a result of the inclusion of stratification in thermal shallow-water theory, which we supported with direct numerical simulations[i].

1. Introduction

The uppermost layer of the ocean, encompassing the region above the main thermocline, including the mixed layer, is marked by the widespread presence of highly energetic mesoscale eddies (20-300 km) with lifespans ranging from weeks to months. These eddies exert a dominant influence on horizontal transport and significantly contribute to vertical transport, thereby impacting the overall biogeochemical cycle [30].

Recent advancements in high-resolution numerical simulations and field observations have shed light on the role of submesoscale motions (1-10 km) in vertical transport dynamics. These motions manifest as Kelvin-Helmholtz-like vortices that form along density fronts and play a significant role in shaping vertical transport processes [29].

Mesoscale motions are well described by quasigeostrophic (QG) theory, valid, roughly speaking, for length scales of the order of the gravest baroclinic (*i.e.*, internal) Rossby radius of deformation and time scales much longer than the inverse of the Coriolis parameter [41]. The simplest QG model, capable to provide a minimal description of mesoscale upper-ocean flow, has a layer of constant density, limited from above by a rigid lid and from below by a soft interface with an infinitely deep layer of quiescent fluid. Using notation introduced by [47], we will refer to this model as the *HLQG* for including a *h*omogeneous (density) *l*ayer. Submesoscale motions, with smaller length scales and faster time scales than mesoscale motions, are, in principle, beyond the scope of QG theory [31]. However, based on numerical simulations, an interesting observation has been recently made by [20], who noted that submesoscale motions can indeed be represented by a QG model with one layer when lateral inhomogeneity is allowed in the buoyancy (temperature) field. Such simulations revealed sub-deformation scale (*i.e.*, submesoscale) Kelvin–Helmholtz-like vortex rolls reminiscent of structures commonly observed in surface ocean color pictures acquired by satellites. A result of a simulation of that type along with an outstanding cloud-free ocean color image revealing submesoscale vortices are shown in Fig. 2.

The above kind of QG model, referred to as *thermal QG model* by [55], has a long history. It was derived by [49] asymptotically from the thermal primitive equations (PE) upon expanding them in small Rossby number. The thermal PE, or rotating shallow-water [55], model was introduced in the 1960s [38], widely employed from the early 1980s through the early 2000s [3, 16, 35, 39, 42, 52], generalized to a system of multiple layers by [46], and extensively investigated theoretically by the same author [47, 48, 50]. Due this author's several contributions, the thermal QG and PE mod-
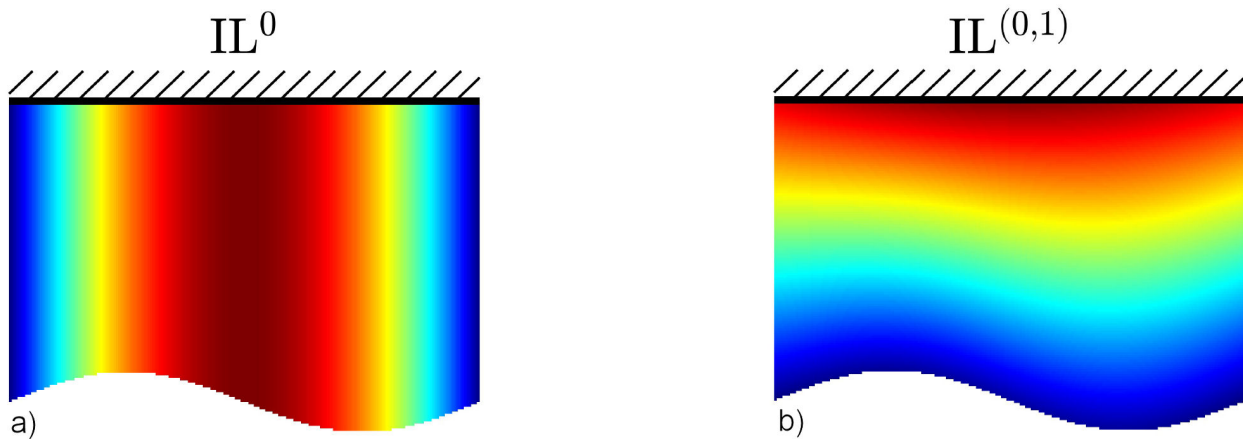
FIGURE 1. Cartoons depicting the density structure on a vertical plane in the thermal shallow-water model, known as Ripa's model or IL^0 a), and its stratified version analyzed in this paper, denoted as $IL^{(0,1)}$ b). A reduced-gravity setting is assumed, featuring one active layer bounded from above by a rigid lid and from below by a soft interface, which interfaces with an inert layer.

els have been referred to as *Ripa's models* [13]. Honoring notation introduced by [47], we will refer to these models as models of the IL^0 class, where "IL" emphasizes that the models have one (or possibly many) *i*nhomogeneous *l*ayer(s) and the superscript indicates that their fields do not vary in the vertical. The left panel of Fig. 1 shows a cartoon of the vertical structure in the IL^0 model class, assuming a reduced-gravity setting.

In the last decade, the IL^0 has made a strong comeback [1, 10, 11, 14, 17, 18, 24, 26, 28, 56], motivated in large part by the tendency of lateral temperature gradients in the upper ocean to become steeper as the ocean absorbs heat from a warming troposphere. In particular, [6] introduced a family of IL-type models, both in PE and for QG dynamics, featuring stratification. The buoyancy field in this model family, referred to as $IL^{(0,n)}$, is written as a polynomial in the vertical coordinate of arbitrary whole degree (n) with coefficients that vary laterally and with time while they are advected (by Lie transport) under the flow of the model horizontal velocity, which is vertically uniform, assigning meaning to the first slot in the superscript in $IL^{(0,n)}$. The $IL^{(0,n)}$PE models admit Euler–Poincaré variational formulation [21] and, via a partial Legendre transform, possess a Lie–Poisson, *i.e.*, non-canonical, Hamiltonian structure [33]. The $IL^{(0,n)}$QG, derived asymptotically from the $IL^{(0,n)}$PE, are Hamiltonian in a Lie–Poisson sense. Including stratification in the IL models expands their scope, for instance, by enabling them to represent important processes such as the restratification of the mixed layer, which follows the development of submesoscale motions by baroclinic instability [5]. (In an attempt to add more physics to the IL models, velocity vertical shear is included in Ref. [47] in the single layer case and in Ref. [7] in a system with multiple layers. However, the resulting IL models with stratification and vertical shear do not enjoy the aforementioned geometric mechanics properties.)

1.1. Goals of the paper

In this paper we investigate in some depth the properties of the recently proposed stratified IL models by focusing on the $IL^{(0,1)}$QG [Fig. 1a)]. We also study how the model fares with respect to baroclinic instability, which, as noted, is an important source of submesoscale circulatory motions in the ocean mixed layer.

It may sound awkward to attempt an investigation of baroclinic instability using an IL model involving a single layer since the (horizontal) velocity is vertically uniform. Two layers may seem to be required as is needed to represent baroclinic instability using the HLQG in the so-called Phillips problem [41]. However, by the thermal-wind balance, which dominates at low frequency, in (every layer of) an IL model the velocity field *implicitly* includes shear in the vertical. Furthermore, implicitly, the velocity vertical profile in the $IL^{(0,1)}$ is curved. This extends the standard baroclinic instability problem of Phillips, or Eady in the continuously stratified case [41], from uniform vertical shear (linear vertical profile) to velocity with vertical curvature, which augments the dimension of the space of parameters for exploration.

While the study of this paper is of interest *per se*, a motivation for pursuing it is found in numerical simulations presented by [6]. These simulations have suggested that inclusion of stratification in the IL models tends to halt the development of submesoscale circulations. This followed from the comparison of evolutions in the IL^0QG and $IL^{(0,1)}$QG forced by bottom topography, which can be included without spoiling the Hamiltonian structure of the models. (This was shown in previous work [8, 20] to hold for the IL^0QG and here we show that it also applies to the $IL^{(0,1)}$QG.) This followed from the comparison of forced evolutions in the IL^0QG and $IL^{(0,1)}$QG. The forcing, which can be interpreted as a topographic forcing [20], does not spoil the Hamiltonian structure
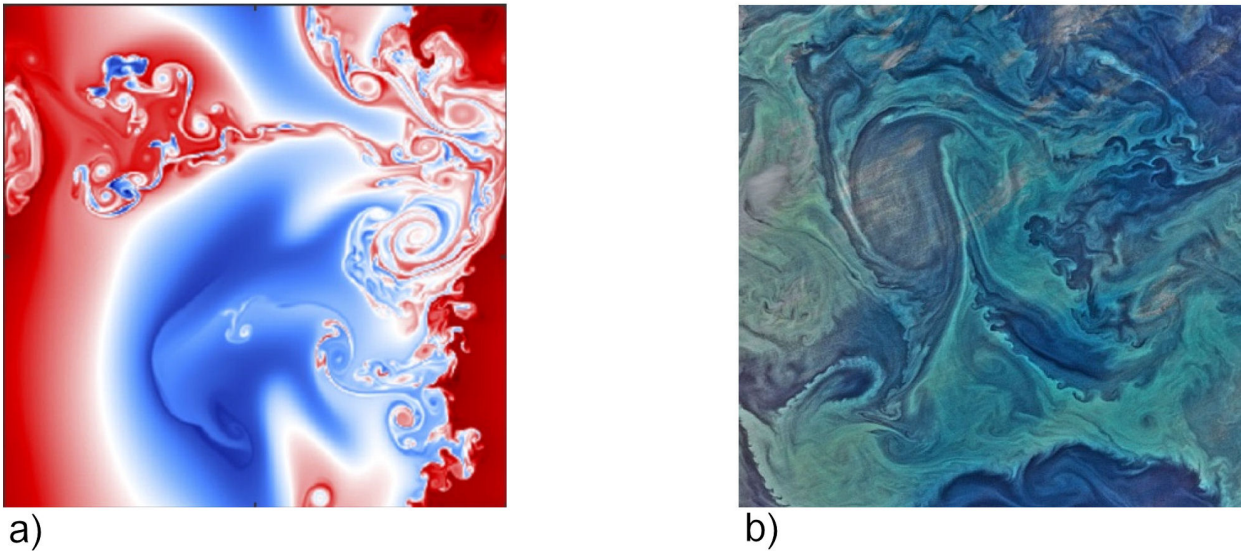
FIGURE 2. a) Emergent cascade of submesoscale vorticity filament rollups in a reduced-gravity direct numerical simulation of the IL^0QG with "topographic" forcing in a doubly periodic domain $\mathbb{R}/R\mathbb{Z} \times \mathbb{R}/R\mathbb{Z}$ of the β-plane, where $R \approx 25$ km is the baroclinic Rossby radius of deformation. b) Ocean color image acquired by VIIRS (Visible Infrared Imaging Radiometer Suite) on 1 January 2015 west of the Drake Passage in the Southern Ocean, revealing vortices with diameters ranging from a couple of km to a couple of hundred km. Image credit: NASA Ocean Color Web (https://oceancolor.gsfc.nasa.gov/gallery/447/).

of the models [8, 20]. The study carried out here will help assess the generality of the numerical evidence presented in Ref. [6].

1.2. Paper organization

The rest of the paper is organized as follows. In Sec. 2 we review the $IL^{(0,1)}QG$ and describe its properties. Specifically, Sec. 2.1 presents the model equations along with its boundary conditions and a physical interpretation of its variables. Section 2.2 discusses uniqueness of solutions in the model. Section 2.3 is dedicated to discussing theorems of circulation, of an appropriately defined Kelvin–Noether-like quantity along material loops (Sec. 2.3.1) and of the velocity along solid boundaries of the flow domain (Sec. 2.3.2). Invariant subspaces of the model are considered in Sec. 2.4. In Sec. 2.5 the Lie–Poisson Hamiltonian structure is clarified, particularly in relation with boundary conditions, which were only superficially discussed in Ref. [6]. Inclusion of topographic forcing without destroying Hamiltonian structure is treated in Sec. 2.6. Reviewing the Hamiltonian structure of the $IL^{(0,1)}QG$ is helpful for Sec. 2.7, which is devoted to describing the conservation laws of the system, which, when linked to explicit symmetries, are obtained via a Noether's theorem appropriate for noncanonical Hamiltonian systems. The conservation laws include a family of integrals of motion that form the kernel of the Lie-Poisson bracket for the potential vorticity evolution independent of buoyancy details as the buoyancy is transported by the flow. Linear waves are discussed in Sec. 3. Section 4 is dedicated to investigate the stability of a baroclinic zonal flow on the β-plane with verti-

cal curvature. Three types of stability notions are discussed, namely, spectral (Sec. 4.1), formal (Sec. 4.2), and Lyapunov (Sec. 4.3). In Sec. 5 we derive a-priori bounds on the nonlinear growth of perturbations to unstable basic states. A discussion, accompanied by direct numerical simulations, of differences between behavior in the $IL^{(0,1)}QG$ and IL^0QG is offered in Sec. 6. Section 7 presents the conclusions from the paper. A glossary containing relevant notions from geophysical fluid dynamics is included following this section. Finally, an Appendix is included containing numerical details of the direct simulations.

2. The $IL^{(0,1)}QG$

Let $\mathbf{x} = (x, y)$ denote position on a periodic zonal domain $\mathscr{D} = \mathbb{R}/L\mathbb{Z} \times [0, W]$ of the β plane. That is, the channel rotates steadily at angular velocity $(1/2)f\hat{\mathbf{z}}$, where $f = f_0 + \beta y$ is the Coriolis parameter. We will denote by $\partial \mathscr{D}_-$ (resp., $\partial \mathscr{D}_+$) the southern (resp., northern) wall of the channel at $y = 0$ (resp., $y = W$). Consider a layer of (ideal) fluid limited above by a horizontally rigid lid at $z = 0$ and below by a soft interface at $z = -h(\mathbf{x}, t)$ with an infinitely deep layer of homogeneous fluid at rest. As in (rotating) shallow-water theory, the motion in the active (top) layer is assumed to be columnar. The vertically shearless horizontal velocity is denoted by $\bar{\mathbf{u}}(\mathbf{x}, t)$, where the overbar represents a vertical average. Similar to conventional *thermal* shallow-water theory, the buoyancy of the active layer is permitted to change both horizontally and temporally [46]. However, unlike this theory, vertical variations in buoyancy are also permitted [6].

In the $\mathrm{IL}^{(0,1)}$ class of *stratified* thermal shallow-water models, of interest here, this is done by writing the buoyancy as

$$\vartheta(\mathbf{x}, z, t) = \bar{\vartheta}(\mathbf{x}, t) + \left(1 + \frac{2z}{h(\mathbf{x}, t)}\right) \vartheta_\sigma(\mathbf{x}, t). \quad (1)$$

That is, the stratification in the active layer is set to be be uniform, with the buoyancy (linearly) varying from $\bar{\vartheta} + \vartheta_\sigma$ at $z = 0$ to $\bar{\vartheta} - \vartheta_\sigma$ at $z = -h$. This imposes the condition

$$\bar{\vartheta} \geq \vartheta_\sigma > 0, \quad (2)$$

i stating that the buoyancy is everywhere positive and the density increases with depth. For future reference, we introduce the instantaneous buoyancy (or Brunt–Väisälä) frequency squared

$$n^2(\mathbf{x}, z, t) := \partial_z \vartheta(\mathbf{x}, z, t) = 2\frac{\vartheta_\sigma(\mathbf{x}, t)}{h(\mathbf{x}, t)}. \quad (3)$$

Remark 1. (On notation). *The subscript notation is motivated by denoting by σ, as in Ref. [47], the scaled vertical coordinate $1 + [2z/h(\mathbf{x}, t)])$. For instance, in the $\mathrm{IL}^{(0,2)}$ model class [6] the buoyancy is written as $\vartheta = \bar{\vartheta} + \sigma\vartheta_\sigma + (\sigma^2 - [1/3])\vartheta_{\sigma^2}$, clarifying additional notation introduced below.*

2.1. Model equations

The evolution equations of the $\mathrm{IL}^{(0,1)}\mathrm{QG}$ in the reduced-gravity setting above are given by [6]

$$\partial_t \bar{\xi} + \left\{\bar{\psi}, \bar{\xi} - R_S^{-2}(\psi_\sigma - \tfrac{2}{3}\psi_{\sigma^2})\right\}_{xy} = 0, \quad (4a)$$

$$\partial_t \psi_\sigma + \{\bar{\psi}, \psi_\sigma\}_{xy} = 0, \quad (4b)$$

$$\partial_t \psi_{\sigma^2} + \{\bar{\psi}, \psi_{\sigma^2}\}_{xy} = 0, \quad (4c)$$

where

$$\nabla^2 \bar{\psi} - R_S^{-2} \bar{\psi} = \bar{\xi} - R_S^{-2}(\psi_\sigma - \tfrac{2}{3}\psi_{\sigma^2}) - \beta y, \quad (4d)$$

with

$$R_S^2 := \left(1 - \tfrac{1}{3}S\right) R^2. \quad (4e)$$

Here

$$\{a, b\}_{xy} := \nabla^\perp a \cdot \nabla b, \quad (4f)$$

for any differentiable functions $a, b(\mathbf{x}, t)$, where $\nabla^\perp$ is short for $\hat{\mathbf{z}} \times \nabla$, is the Jacobian of the transformation $(x, y) \mapsto (a, b)$ and

$$R := \frac{\sqrt{g_\mathrm{r} H_\mathrm{r}}}{|f_0|}, \quad S := \frac{N_\mathrm{r}^2 H_\mathrm{r}}{2g_\mathrm{r}}. \quad (4g)$$

The positive constants H_r, g_r, and N_r^2 are reference (*i.e.*, in the absence of currents) layer thickness, vertically averaged buoyancy,[ii] and buoyancy frequency squared, respectively. The (positive) constant on the left in Eq. (4g) corresponds to

the equivalent barotropic (external) Rossby radius of deformation in a model with arbitrary stratification in a reduced-gravity setting. The constant on the right in Eq. (4g) is a measure of reference stratification. The reference buoyancy varies from $1 + S$ at $z = 0$ to $1 - S$ at $z = -H_\mathrm{r}$. Thus, by static stability, $0 < S < 1$.

The system is subjected to

$$\nabla^\perp \bar{\psi} \cdot \hat{\mathbf{n}}|_{\partial \mathscr{D}_\pm} = 0 \iff \partial_x|_{y=0,W} \bar{\psi} = 0, \quad (5a)$$

and periodicity in the along channel direction, x, *i.e.*,

$$\bar{\xi}(x + L, y, t) = \bar{\xi}(x, y, t), \quad (5b)$$

and similarly for the rest of the variables.

The $\mathrm{IL}^{(0,1)}\mathrm{QG}$ has three prognostic fields, $(\bar{\xi}, \psi_\sigma, \psi_{\sigma^2})$, assumed to be sufficiently smooth in each of its arguments, $(\mathbf{x}, t)$. These diagnose $\bar{\psi}(\mathbf{x}, t)$ via (4d), which defines the invertibility principle for the $\mathrm{IL}^{(0,1)}\mathrm{QG}$. (In Fourier space, say, the positive-definite symmetric operator $R_S^{-2} - \nabla^2$ is non-degenerate; hence, its operator inverse $(R_S^{-2} - \nabla^2)^{-1}$ exists and is well defined.)

The physical meaning of the above variables is as follows. Let $\mathrm{Ro} > 0$ be a small parameter taken to represent a Rossby number, measuring the strength of inertial and Coriolis forces, *e.g.*,

$$\mathrm{Ro} = \frac{V}{|f_0|R} \ll 1, \quad (6)$$

where V is a characteristic velocity. In QG theory [41] it is assumed that

$$(|\bar{\mathbf{u}}|, h - H_\mathrm{r}, \partial_t, \beta y) = O(\mathrm{Ro}V, \mathrm{Ro}R, \mathrm{Ro}f_0, \mathrm{Ro}f_0). \quad (7)$$

Consistent with the QG scaling (7), with an $O(\mathrm{Ro}^2)$ error, one has:

$$\bar{\mathbf{u}} = \nabla^\perp \bar{\psi}, \quad (8)$$

$$h = H_\mathrm{r} + \frac{H_\mathrm{r}}{f_0 R_S^2}(\bar{\psi} - \psi_\sigma + \tfrac{2}{3}\psi_{\sigma^2}), \quad (9)$$

$$\bar{\vartheta} = g_\mathrm{r} + \frac{2g_\mathrm{r}}{f_0 R^2}\psi_\sigma, \quad (10)$$

$$\vartheta_\sigma = \tfrac{1}{2}N_\mathrm{r}^2 H_\mathrm{r} + \frac{4g_\mathrm{r}}{f_0 R^2}\psi_{\sigma^2}, \quad (11)$$

where

$$\frac{\psi_\sigma - 2\psi_{\sigma^2}}{f_0 R^2} \geq \frac{S - 1}{2}, \quad \frac{\psi_{\sigma^2}}{f_0 R^2} > -\frac{S}{4}, \quad (12)$$

by (2). Finally, with an $O(\mathrm{Ro}^2)$ error,

$$\frac{\nabla^\perp \cdot \bar{\mathbf{u}} + f}{h} = \frac{f_0 + \bar{\xi}}{H_\mathrm{r}}. \quad (13)$$

The left-hand-side of (13) is proportional to the Ertel z/h-potential vorticity in the hydrostatic approximation and with the horizontal velocity replaced with $\bar{\mathbf{u}}$ [47]. Thus $\bar{\xi}$ can be identified with potential vorticity in the $\mathrm{IL}^{(0,1)}\mathrm{QG}$.

With the identifications (8)–(13), Eq. (4a) controls the evolution of $IL^{(0,1)}QG$ potential vorticity. This quantity is not materially conserved, *i.e.*, advected (by Lie transport) under the flow of $\nabla^\perp \bar{\psi}$. Rather, the potential vorticity in the $IL^{(0,1)}QG$ is created (or annihilated) by the misalignment between the gradients of layer thickness and buoyancy (cf. Sec. 2.3.1, for additional discussion). This is consistent with Ertel's z/h-potential vorticity not being materially conserved. Equations (4b) and (4c) control, respectively, the evolution of the vertical average and gradient of buoyancy. These are both materially conserved. Altogether (4b) and (4c) give material conservation of buoyancy in the $IL^{(0,1)}QG$. Finally, the boundary condition (5a) means no flow through the solid walls of the zonal channel domain.

Remark 2. (Implicit vertical shear) *By the thermal-wind balance, the velocity has implicit vertical curvature, which motivates the streamfunction notations ψ_σ and ψ_{σ^2} [6]. Indeed, the buoyancy distribution* (1) *implicitly implies that the velocity is determined, with an $O(\mathrm{Ro}^2)$ error, by the streamfunction*

$$\psi = \bar{\psi} + \left(1 + \frac{2z}{H_r}\right)\psi_\sigma + \left(\left[1 + \frac{2z}{H_r}\right]^2 - \frac{1}{3}\right)\psi_{\sigma^2}. \quad (14)$$

We note that the $IL^0 QG$ can be recovered from system (41) upon omitting ψ_{σ^2} and setting $S = 0$, *i.e.*, replacing R_S with R. Note, for instance, that the buoyancy restriction in the $IL^0 QG$ is $\psi_\sigma > -(1/2)f_0 R^2$. The potential vorticity in the $IL^0 QG$, given by $\bar{\xi} = \nabla^2 \bar{\psi} - R^{-2}(\bar{\psi} - \psi_\sigma) + \beta y$, is created (or annihilated) as in the $IL^{(0,1)}QG$ due to lateral changes in buoyancy, which is only permitted to vary in the horizontal (and time). This is unlike the HLQG, which follows from the $IL^0 QG$ after ignoring ψ_σ. The potential vorticity in the HLQG, $\bar{\xi} = \nabla^2 \bar{\psi} - R^{-2}\bar{\psi} + \beta y$, is materially conserved. The results discussed below for the $IL^{(0,1)}QG$ can be translated to corresponding results for the $IL^0 QG$ or HLQG in the indicated limits.

2.2. Uniqueness of solutions

Assume that $\bar{\psi}_1(\mathbf{x}, t)$ and $\bar{\psi}_2(\mathbf{x}, t)$ are two solutions of (4d), on the zonal channel domain $\mathscr{D}$, each one satisfying boundary conditions (5). Let $\phi := \bar{\psi}_1 - \bar{\psi}_2$; then

$$\nabla^2 \phi - R_S^{-2}\phi = 0, \quad (15)$$

on $\mathscr{D}$ subjected to

$$\nabla^\perp \phi \cdot \hat{\mathbf{n}}|_{\partial \mathscr{D}_\pm} = 0 \iff \partial_x|_{y=0,W}\phi = 0,$$

$$\phi(x, 0, t) = \phi(x, L, t). \quad (16)$$

Multiplying (15) by ϕ and integrating by parts with (16) in mind,

$$\int_{\mathscr{D}} |\nabla\phi|^2 + R_S^{-2}\phi^2 \, d^2x = 0, \quad (17)$$

which holds if and only if $\phi = 0$, *i.e.*, $\psi_1 = \psi_2$.

2.3. Circulations

2.3.1. A Kelvin circulation theorem

Let $\mathbf{f}(\mathbf{x})$ be such that $\nabla^\perp \cdot \mathbf{f} = \beta y$. Let in addition $\partial \mathscr{D}_t$ be the material loop enclosing a material region $\mathscr{D}_t$ at time $t > 0$ after being advected from its initial position at time $t = 0$ by the flow of $\nabla^\perp \bar{\psi}$. Consider

$$\mathcal{K} := \oint_{\partial \mathscr{D}_t} (\nabla^\perp \bar{\psi} + \mathbf{f} - R_S^{-2}\nabla^{-2}\nabla^\perp$$

$$\times [\bar{\psi} - \psi_\sigma + \{2/3\}\psi_{\sigma^2}]) \cdot d\mathbf{x} = \int_{\mathscr{D}_t} \bar{\xi} \, d^2x, \quad (18)$$

where the last equality follows upon using Stokes' theorem. The above is an appropriate definition of the *Kelvin circulation for the $IL^{(0,1)}QG$* as it leads to a theorem analogous to the Kelvin–Noether theorem for the $IL^{(0,1)}PE$ [6]. It extends that one found in Sec. 3.1 of [23] for adiabatic (*i.e.*, HL) QG dynamics to stratified thermal (*i.e.*, $IL^{(0,1)}$) QG dynamics. By (4a) and after pulling back the integrand in the last equality of (18) to $t = 0$ and changing variables, it follows that

$$\dot{\mathcal{K}} = R_S^{-2}\int_{\mathscr{D}_t}\left\{\bar{\psi}, \psi_\sigma - \tfrac{2}{3}\psi_{\sigma^2}\right\}_{xy} d^2x. \quad (19)$$

As in the $IL^{(0,1)}PE$, the misalignment between the gradients of layer thickness and buoyancy creates (or destroys) Kelvin circulation. This is most cleanly seen by noting that

$$\int_{\mathscr{D}_t} \nabla^\perp h \cdot \nabla\left(\bar{\vartheta} - \tfrac{1}{3}\vartheta_\sigma\right) d^2x$$

$$= 2R_S^{-2}\int_{\mathscr{D}_t}\left\{\bar{\psi}, \psi_\sigma - \tfrac{2}{3}\psi_{\sigma^2}\right\}_{xy} d^2x \quad (20)$$

with an $O(\mathrm{Ro}^3)$ error.

Remark 3. *Two exceptions are the cases when $\partial \mathscr{D}_t$ is isopycnic at each level in the vertical and when this is solid, as is the case of the boundary of the zonal channel domain $\mathscr{D}$. In each of these situations, the Kelvin circulation is conserved. The former follows by noting that the right-hand side of* (19) *equals $-\oint_{\partial \mathscr{D}_t}\bar{\psi}\nabla^\perp(\psi_\sigma - [2/3]\psi_{\sigma^2}) \cdot \hat{\mathbf{n}}ds$, while the latter follows by realizing that it is also equal to $\oint_{\partial \mathscr{D}_t}(\psi_\sigma - [2/3]\psi_{\sigma^2})\nabla^\perp\bar{\psi} \cdot \hat{\mathbf{n}}ds$. Kelvin circulation conservation, when $\partial \mathscr{D}_t$ is solid, differs from that in the $IL^{(0,1)}PE$, where it must be levelwise isopycnic, making the $IL^{(0,1)}QG$ less restrictive than the $IL^{(0,1)}PE$.*

Note that $\{\bar{\psi}, \psi_\sigma - [2/3]\psi_{\sigma^2}\}_{xy} = \nabla^\perp\bar{\psi} \cdot \nabla(\psi_\sigma - [2/3]\psi_{\sigma^2}) = -\nabla\bar{\psi} \cdot \nabla^\perp(\psi_\sigma - [2/3]\psi_{\sigma^2})$. Since $\nabla \cdot \nabla^\perp = 0$, then by Stokes' theorem the integral on the right-hand side of (19) is equal to $-\oint_{\partial \mathscr{D}_t}\bar{\psi}\nabla^\perp(\psi_\sigma - [2/3]\psi_{\sigma^2}) \cdot \hat{\mathbf{n}}ds$. This vanishes if ψ_σ and ψ_{σ^2} are constant along $\mathscr{D}_t$. The Kelvin circulation is conserved in these circumstances, which express that the material loop $\partial \mathscr{D}_t$ is isopycnic at each level in the vertical.

When $\mathscr{D}_t$ is replaced by the zonal channel domain $\mathscr{D}$, then the Kelvin circulation is conserved, whether $\partial\mathscr{D}$ is levelwise isopycnic or not. To see this, first note that, in such a case, the integral on right-hand side of (19) is replaced by $\int_{\mathscr{D}}\{\bar{\psi}, R_S^{-2}(\psi_\sigma - [2/3]\psi_{\sigma^2}) - \bar{\xi}\}_{xy}\,d^2x$. By (5b) this is equal to $(\int_{\partial\mathscr{D}_-} - \int_{\partial\mathscr{D}_+})(R_S^{-2}(\psi_\sigma - [2/3]\psi_{\sigma^2}) - \bar{\xi})\nabla^\perp\bar{\psi}\cdot\hat{\mathbf{n}}ds$, upon invoking Stokes' theorem. By (5b) each term of this sum individually vanishes. This is unlike the $\text{IL}^{(0,1)}\text{PE}$, in which case $\partial\mathscr{D}_\pm$ must be levelwise isopycnic, making the $\text{IL}^{(0,1)}\text{QG}$ less restrictive than the $\text{IL}^{(0,1)}\text{PE}$. (In that model and the present one, if this condition is imposed initially, then it is preserved for all time).

2.3.2. Circulation of the velocity

Consider

$$\gamma_\pm := \int_{\partial\mathscr{D}_\pm} \nabla\bar{\psi}\cdot\hat{\mathbf{n}}ds = \int_0^L \partial_y|_{y=0,W}\bar{\psi}\,dx, \qquad (21)$$

defining the *velocity circulations* along the coasts of the zonal channel domain. Note the difference with (18), which we have referred to as a Kelvin circulation for the $\text{IL}^{(0,1)}\text{QG}$. We will *impose* the condition

$$\dot{\gamma}_\pm = 0. \qquad (22)$$

Constancy of $\gamma_\pm$ is a boundary condition, in addition to (5), which *guarantees* energy preservation (cf. Sec. 2.7.1). This is not a peculiarity of the $\text{IL}^{(0,1)}\text{QG}$, but a rather general aspect of QG models.

2.4. Invariant subspaces

If system (4) is initialized from ψ_σ, $\psi_{\sigma^2} = \text{const}$, then these variables preserve their initial constant values at all times. In other words, the subspace $\{\psi_\sigma, \psi_{\sigma^2} = \text{const}\}$ is an invariant subspace of the $\text{IL}^{(0,1)}\text{QG}$. The dynamics on this invariant subspace is formally the same as that in the adiabatic case, that is, the HLQG, wherein the potential vorticity, given by $\bar{\xi} = \nabla^2\bar{\psi} - R^{-2}\bar{\psi} + \beta y$, is materially conserved. This holds formally because ψ_{σ^2} actually is a perturbation on a reference uniform stratification. But this is reflected in Eq. (4) only through the stratification parameter S. The HLQG and $\text{IL}^{(0,1)}\text{QG}$ potential vorticities on $\{\psi_\sigma, \psi_{\sigma^2} = \text{const}\}$ differ by unimportant constants and by the Rossby radius of deformation being smaller for $S \neq 0$. In turn, if (4) is initialized from $\psi_{\sigma^2} = \text{const}$, then this is preserved for all time. The dynamics on this invariant subspace is formally the same as that of the IL^0QG, with the caveats noted above. Similarly, in the IL^0QG, obtained from the $\text{IL}^{(0,1)}\text{QG}$ by ignoring ψ_{σ^2} and setting $S = 0$, the subspace $\{\psi_\sigma = \text{const}\}$ is invariant and on this invariant subspace the dynamics coincides with that of the HLQG, exactly in this case.

2.5. Hamiltonian structure

We begin with a definition that is helpful to understand operations in the rest of the paper. This is followed by an assump-

tion, which enables us to frame the Hamiltonian structure of the $\text{IL}^{(0,1)}\text{QG}$ in a domain with boundaries consistent with the aforementioned definition.

Definition 1. (Functional, functional derivatives, and variations). *A functional $\mathcal{F}$ of scalar fields $\varphi^j(\mathbf{x}, t)$, $j = 1, \ldots, J$, denoted $\mathcal{F}[\varphi]$, is a map from a vector space V to $\mathbb{R}$. The functional derivatives of $\mathcal{F}$ are defined as the unique elements $\delta\mathcal{F}/\delta\varphi^j$, $j = 1, \ldots, J$, satisfying*

$$\frac{d}{d\varepsilon}\bigg|_{\varepsilon=0}\mathcal{F}[\varphi + \varepsilon\delta\varphi] =: \sum_{j=1}^J \int_{\mathscr{D}} \frac{\delta\mathcal{F}}{\delta\varphi^j}\delta\varphi^j\,d^2x$$

$$=: \delta\mathcal{F}[\delta\varphi; \varphi], \qquad (23)$$

where ε is a real parameter and $\delta\varphi$ is called the variation of φ. The functional $\delta\mathcal{F}$, linear in $\delta\varphi$, is called the first variation of $\mathcal{F}$. The above is the Gateaux definition of functional derivative. The second variation of $\mathcal{F}$, quadratic in $\delta\varphi$,

$$\delta^2\mathcal{F}[\delta\varphi; \varphi] := \frac{d^2}{d\varepsilon^2}\bigg|_{\varepsilon=0}\mathcal{F}[\varphi + \varepsilon\delta\varphi]$$

$$=: \sum_{j,k=1}^J \int_{\mathscr{D}} \frac{\delta^2\mathcal{F}}{\delta\varphi^j\delta\varphi^k}\delta\varphi^j\delta\varphi^k\,d^2x, \qquad (24)$$

where $\delta^2\mathcal{F}/\delta\varphi^j\delta\varphi^k$, $i,k = 1, \ldots, J$, define the second functional derivatives of $\mathcal{F}$. Higher-order variations, as well as functional derivatives, are similarly defined, so that the total variation of $\mathcal{F}$,

$$\Delta\mathcal{F}[\delta\varphi; \varphi] := \mathcal{F}[\varphi + \delta\varphi] - \mathcal{F}[\varphi] = \delta\mathcal{F}[\delta\varphi; \varphi]$$

$$+ \frac{1}{2!}\delta^2\mathcal{F}[\delta\varphi; \varphi] + \frac{1}{3!}\delta^3\mathcal{F}[\delta\varphi; \varphi] + \cdots, \quad (25)$$

where $\delta^n\mathcal{F} = O(\|\delta\varphi\|^n)$ with $\|\cdot\|^2 = \int_{\mathscr{D}}(\cdot)^2\,d^2x$ is the square of the L^2 norm.

Assumption 1. *We will assume that all variations in the sense of Definition 1 are restricted to those that preserve the circulation of the velocity along each wall of the zonal channel domain, namely,*

$$\delta\gamma_\pm = 0. \qquad (26)$$

The restriction (26) enables a Hamiltonian formulation of the $\text{IL}^{(0,1)}\text{QG}$ wherein variational calculus is consistent with Definition 1. Otherwise, the space space variables must be augmented to include $\gamma_\pm$ as done in [22]. However, this requires one to define the notion of variational derivative differently than in Definition 1 [27].

Remark 4. *While allowing variations of $\gamma_\pm$ adds generality to the Hamiltonian formulation of the $\text{IL}^{(0,1)}\text{QG}$, the practical consequences of such added generality are minimal. This is illustrated in Ref. [45] for the stability problem.*

Let

$$\mathcal{E}[\bar{\xi}, \psi_\sigma, \psi_{\sigma^2}] := \frac{1}{2} \int_{\mathscr{D}} |\nabla \bar{\psi}|^2 + R_S^{-2} \bar{\psi}^2 \, d^2x = -\frac{1}{2} \int_{\mathscr{D}} \bar{\psi} \left(\bar{\xi} - R_S^{-2} \left(\psi_\sigma - \tfrac{2}{3} \psi_{\sigma^2} \right) - \beta y \right) \, d^2x, \tag{27}$$

be the energy, where the equality follows from (5) upon integration by parts. That $\mathcal{E}$ indeed is a functional of $(\bar{\xi}, \psi_\sigma, \psi_{\sigma^2})$ follows by noting that

$$\bar{\psi} = (\nabla^2 - R_S^{-2})^{-1} \left(\bar{\xi} - R_S^{-2}(\psi_\sigma - \tfrac{2}{3}\psi_{\sigma^2}) - \beta y \right), \tag{28}$$

where $(\nabla^2 - R_S^{-2})^{-1}$ is interpreted in terms of the relevant Green's function of the elliptic problem (4d).

Now, consider

$$\{\mathcal{F}, \mathcal{G}\} := \int_{\mathscr{D}} \begin{pmatrix} \frac{\delta \mathcal{F}}{\delta \bar{\xi}} \\ \frac{\delta \mathcal{F}}{\delta \psi_\sigma} \\ \frac{\delta \mathcal{F}}{\delta \psi_{\sigma^2}} \end{pmatrix}^\top \begin{pmatrix} -\{\bar{\xi}, \cdot\}_{xy} & -\{\psi_\sigma, \cdot\}_{xy} & -\{\psi_{\sigma^2}, \cdot\}_{xy} \\ -\{\psi_\sigma, \cdot\}_{xy} & 0 & 0 \\ -\{\psi_{\sigma^2}, \cdot\}_{xy} & 0 & 0 \end{pmatrix} \begin{pmatrix} \frac{\delta \mathcal{G}}{\delta \bar{\xi}} \\ \frac{\delta \mathcal{G}}{\delta \psi_\sigma} \\ \frac{\delta \mathcal{G}}{\delta \psi_{\sigma^2}} \end{pmatrix} d^2x$$

$$= \int_{\mathscr{D}} \bar{\xi} \left\{ \frac{\delta \mathcal{F}}{\delta \bar{\xi}}, \frac{\delta \mathcal{G}}{\delta \bar{\xi}} \right\}_{xy} + \sum_{n=1}^{2} \psi_{\sigma^n} \left(\left\{ \frac{\delta \mathcal{F}}{\delta \bar{\xi}}, \frac{\delta \mathcal{G}}{\delta \psi_{\sigma^n}} \right\}_{xy} + \left\{ \frac{\delta \mathcal{F}}{\delta \psi_{\sigma^n}}, \frac{\delta \mathcal{G}}{\delta \bar{\xi}} \right\}_{xy} \right) d^2x \tag{29}$$

for any $\mathcal{F}, \mathcal{G}[\bar{\xi}, \psi_\sigma, \psi_{\sigma^2}]$, where the second equality follows upon integrating parts and requiring

$$\nabla^\perp \frac{\delta \mathcal{F}}{\delta \bar{\xi}} \cdot \hat{\mathbf{n}}|_{\partial \mathscr{D}_\pm} = 0, \quad \nabla^\perp \frac{\delta \mathcal{F}}{\delta \psi_\sigma} \cdot \hat{\mathbf{n}}|_{\partial \mathscr{D}_\pm} = 0, \quad \nabla^\perp \frac{\delta \mathcal{F}}{\delta \psi_{\sigma^2}} \cdot \hat{\mathbf{n}}|_{\partial \mathscr{D}_\pm} = 0, \tag{30}$$

for all $\mathcal{F}[\bar{\xi}, \psi_\sigma, \psi_{\sigma^2}]$. It should be noted that periodicity in x accounts for the vanishing of the corresponding flux integral across the (oriented) boundary piece $\partial \tilde{\mathscr{D}} := \partial \mathscr{D} \setminus \partial \mathscr{D}_- \cup \partial \mathscr{D}_+$. Explicitly, these integrals are of the form $\int_{\partial \tilde{\mathscr{D}}} ab\nabla^\perp c \cdot \hat{\mathbf{n}} ds$, where $a, b, c(\mathbf{x}, t)$ are x-periodic. Noting that $\mathbf{n} ds = -d\mathbf{x}^\perp$, one computes $\int_{\partial \tilde{\mathscr{D}}} ab\nabla^\perp c \cdot \hat{\mathbf{n}} ds = \int_0^W ab(-\partial_y c)|_{x=L} dy + \int_W^0 ab(-\partial_y c)|_{x=0} dy = \int_0^W \left(ab\partial_y c|_{x=0} - ab\partial_y c|_{x=L} \right) dy = 0$.

For all $\mathcal{F}, \mathcal{G}, \mathcal{H}[\bar{\xi}, \psi_\sigma, \psi_{\sigma^2}]$, the bracket defined in Eq. (29) satisfies: $\{\mathcal{F} + \mathcal{G}, \mathcal{H}\} = \{\mathcal{F}, \mathcal{H}\} + \{\mathcal{G}, \mathcal{H}\}$ (bilinearity); $\{\mathcal{F}, \mathcal{G}\} = -\{\mathcal{G}, \mathcal{F}\}$ (antisymmetry); $\{\{\mathcal{F}, \mathcal{G}\}, \mathcal{H}\} + \circlearrowleft = 0$ (Jacobi identity); and $\{\mathcal{F}\mathcal{G}, \mathcal{H}\} = \mathcal{F}\{\mathcal{G}, \mathcal{H}\} + \{\mathcal{F}, \mathcal{H}\}\mathcal{G}$ (Leibniz rule). An explicit proof of the Jacobi identity is given in Ref. [6]. These properties make $\{ , \}$ a Poisson bracket and by its linear dependence on $(\bar{\xi}, \psi_\sigma, \psi_{\sigma^2})$ it is classified as of Lie–Poisson type. Such noncanonical brackets inherit the properties above from analogous properties of $\{ , \}_{xy}$, the canonical bracket in $\mathbb{R}^2$.

Since

$$\delta \mathcal{E} = - \int_{\mathscr{D}} \bar{\psi} \delta \bar{\xi} + R_S^{-2} \bar{\psi} \delta \psi_\sigma + \tfrac{2}{3} R_S^{-2} \bar{\psi} \delta \psi_{\sigma^2} \, d^2x, \tag{31}$$

where the boundary terms have cancelled out by Assumption 1, it follows that

$$\frac{\delta \mathcal{E}}{\delta \bar{\xi}} = -\bar{\psi}, \quad \frac{\delta \mathcal{E}}{\delta \psi_\sigma} = R_S^{-2} \bar{\psi}, \quad \frac{\delta \mathcal{E}}{\delta \psi_{\sigma^2}} = -\tfrac{2}{3} R_S^{-2} \bar{\psi}. \tag{32}$$

Equations (4a)–(4b) then follow as

$$\partial_t \bar{\xi} = \{\bar{\xi}, \mathcal{E}\}, \quad \partial_t \psi_\sigma = \{\psi_\sigma, \mathcal{E}\}, \quad \partial_t \psi_{\sigma^2} = \{\psi_{\sigma^2}, \mathcal{E}\}. \tag{33}$$

In other words, the $\mathrm{IL}^{(0,1)}\mathrm{QG}$ model constitutes a Lie–Poisson Hamiltonian system in the variables $(\bar{\xi}, \psi_\sigma, \psi_{\sigma^2})$ with Hamiltonian given by (27) and Lie–Poisson bracket defined by (29). More generally, one has

$$\dot{\mathcal{F}} = \{\mathcal{F}, \mathcal{E}\}, \tag{34}$$

for all $\mathcal{F}[\bar{\xi}, \psi_\sigma, \psi_{\sigma^2}]$.

The $\mathrm{IL}^0\mathrm{QG}$ is also Lie–Poisson Hamiltonian, with Hamiltonian given by (27) with R_S replaced by R and Lie–Poisson bracket given by (29) with ψ_{σ^2} ignored. The resulting bracket is found in Ref. [55], which is a particular version of the one derived by [49] for a system more general than the $\mathrm{IL}^0\mathrm{QG}$. A (Lie–Poisson) deformation of the $\mathrm{IL}^0\mathrm{QG}$ bracket, *i.e.*, with the same kernel (cf. Sec. 2.7), appears in Ref. [19]. Interestingly, low-β magnetohydrodynamics [34] and incompressible, nonhydrostatic, Boussinesq fluid dynamics on a vertical plane share this bracket [4].

For a geometric mechanics interpretation of the $\mathrm{IL}^{(0,1)}\mathrm{QG}$, where its Lie–Poisson bracket (29) is associated with the Lie algebra of the group of area-preserving diffeomorphisms extended by a semidirect product with that of the vector field formed by two copies of the space of smooth functions—this arising from broken symmetry—the interested reader is referred to [9].

2.6. Topographic forcing

Let $\psi_0(\mathbf{x})$ be an arbitrary scalar function on the zonal channel domain $\mathscr{D}$ of length-squared-over-time units, conveniently assumed to satisfy $\nabla \psi_0 \times \hat{\mathbf{n}}|_{\partial \mathscr{D}} = 0$. Let $L_0 = \text{const}$ have

units of length. The Lie–Poisson Hamiltonian structure of the $\mathrm{IL}^{(0,1)}$QG is not spoiled if (41a) is modified as

$$\partial_t \bar{\xi} + \{\bar{\psi}, \bar{\xi} - R_S^{-2}(\psi_\sigma - \tfrac{2}{3}\psi_{\sigma^2})\}_{xy}$$
$$= L_0^{-2}\{\psi_0, \psi_\sigma - \tfrac{2}{3}\psi_{\sigma^2}\}_{xy}. \quad (35)$$

The term on the right-hand side of (35) may be viewed as forcing resulting from imposing an irregular topography on the rigid lid separating the active layer from the atmosphere above. This extends an earlier [20] interpretation of a similar term in the case where the active layer rests on bottom topography while having a free top boundary with the atmosphere. System (41) with (41a) replaced with (35) is obtained from the Lie–Poisson bracket (29) with the Hamiltonian given by

$$\mathcal{E}_0[\bar{\xi}, \psi_\sigma, \psi_{\sigma^2}] := \frac{1}{2}\int_{\mathscr{D}} |\nabla\bar{\psi}|^2 + R_S^{-2}\bar{\psi}^2$$
$$- 2L_0^{-2}\psi_0(\psi_\sigma - \tfrac{2}{3}\psi_{\sigma^2})\, d^2x. \quad (36)$$

The change of the Kelvin circulation $\mathcal{K}$ along a material loop $\partial\mathscr{D}_t$ is given by $\int_{\mathscr{D}_t}[R_S^{-2}\bar{\psi} + L_0^{-2}\psi_0, \psi_\sigma - (2/3)\psi_{\sigma^2}]\, d^2x$, rather than (19). As in the unforced case, *i.e.*, with $L = 0$, $\mathcal{K}$ is conserved when $\partial\mathscr{D}_t$ is levelwise isopycnic and along the walls $\partial\mathscr{D}_\pm$ of $\mathscr{D}$.

2.7. Conservation laws

2.7.1. Energy, zonal momentum, and Casimirs

The noncanonical Hamiltonian formalism enables the connection of conservation laws with symmetries through *Noether's theorem* as follows:

Theorem 1. (Noether for noncanonical Hamiltonians). *Let P be a* Poisson manifold, *i.e., an infinite-dimensional smooth manifold endowed with a Poisson bracket or structure* $\{\,,\}: C^\infty(P) \times C^\infty(P) \to C^\infty(P)$. *The evolution of any functional* $\mathcal{F}[\varphi] \in C^\infty(P) : P \to \mathbb{R}$ *is controlled by* $\dot{\mathcal{F}} = \{\mathcal{F}, \mathcal{E}\}$ *with the dynamics specified by* $\mathcal{E}[\varphi]$, *the Hamiltonian. Consider the one-parameter family of variations induced by a functional* $\mathcal{G}[\varphi]$ *defined by* $\delta_{\mathcal{G}} := -\varepsilon\{\mathcal{G}, \cdot\}$, *where* $\varepsilon > 0$ *is small. The change induced by* $\mathcal{G}$ *on* $\mathcal{E}$ *is*

$$\Delta_{\mathcal{G}}\mathcal{E} := \mathcal{E}[\varphi + \delta_{\mathcal{G}}\varphi] - \mathcal{E}[\varphi] \sim \varepsilon\{\mathcal{E}, \mathcal{G}\} = -\varepsilon\dot{\mathcal{G}}, \quad (37)$$

where $\sim$ *means asymptotically as* $\varepsilon \downarrow 0$. *Moreover,*

$$\frac{d}{dt}\Delta_{\mathcal{G}}\mathcal{F} - \Delta_{\mathcal{G}}\frac{d\mathcal{F}}{dt} \sim \varepsilon\left\{\mathcal{F}, \frac{d\mathcal{G}}{dt}\right\}, \quad (38)$$

for any $\mathcal{F}[\varphi]$. *The following holds:*

1. *Symmetry of* $\mathcal{E}$ *under the transformation induced by* $\mathcal{G}$ *implies conservation of* $\mathcal{G}$ *and vice versa.*

2. *If* $\mathcal{G}$ *is an integral of motion, then the transformation generated by* $\mathcal{G}$ *represents a symmetry in the general sense that the result of making a transformation and letting the time run is independent of the order in which these operations are performed.*

A statement of Theorem 1(i) can be found in [54]. Theorem 1(ii) is due to [44]. In both cases, if $\mathcal{G}$ is conserved, then it transforms solutions into solutions, *i.e.*, $\partial_t\varphi = \{\varphi, \mathcal{E}\}$ transforms into $\partial_t\Delta_{\mathcal{G}}\varphi = \Delta_{\mathcal{G}}\partial_t\varphi = \Delta_{\mathcal{G}}\{\varphi, \mathcal{E}\} = \{\Delta_{\mathcal{G}}\varphi, \mathcal{E}\}$ under the transformation induced by $\mathcal{G}$.

Note that $-\mathcal{E}$ is the generator of time shifts $t \to t-\varepsilon$ since $\delta_{-\mathcal{E}}\varphi = \varepsilon\{\mathcal{E}, \varphi\} = -\varepsilon\partial_t\varphi$. By Theorem 1(i), conservation of $\mathcal{E}$ is related to symmetry of $\mathcal{E}$ under selfinduced transformations, as is the case of the $\mathrm{IL}^{(0,1)}$QG's energy, given in (27). Let $\mathcal{M}[\varphi]$, identified with the *zonal momentum*, be defined as the generator of the transformation $x \to x - \varepsilon$. That is, $\delta_{\mathcal{M}}\varphi = -\varepsilon\{\mathcal{M}, \varphi\} := -\varepsilon\partial_x\varphi$, which is satisfied in the $\mathrm{IL}^{(0,1)}$QG, *i.e.*, with $\varphi = (\bar{\xi}, \psi_\sigma, \psi_{\sigma^2})$ and bracket (29), by

$$\mathcal{M}[\bar{\xi}, \psi_\sigma, \psi_{\sigma^2}] = \int_{\mathscr{D}} y\bar{\xi}\, d^2x. \quad (39)$$

Theorem 1(i) links constancy of $\mathcal{M}$ with symmetry of the $\mathrm{IL}^{(0,1)}$QG's energy (27) under zonal translations.

By Theorem 1(ii), conservation of $\mathcal{E}$ and $\mathcal{M}$ imply that the transformations they induced on any functional represents a symmetry in the general sense that transforming and letting the time run commute. But the reciprocal of the latter is not strictly true. Indeed, if the left-hand-side of (38) vanishes, then $\dot{\mathcal{G}} = 0$ is equal to a *distinguished function*. Namely, a function of functionals $\mathcal{C}[\varphi]$, called *Casimirs*, which are nontrivial solutions of

$$\{\mathcal{F}, \mathcal{C}\} = 0\,\forall\mathcal{F}. \quad (40)$$

The Casimirs form the kernel of $\{\,,\}$ and, since $\mathcal{F}$ includes $\mathcal{E}$, they represent integrals of motion. However, they do not generate any variation, *i.e.*, $\delta_{\mathcal{C}}\varphi = -\varepsilon\{\mathcal{C}, \varphi\} = 0$, and thus are not related to explicit symmetries, *i.e.*, symmetries that are visible in the Eulerian variables that form the phase space in which the dynamics are being viewed. The Casimirs of the $\mathrm{IL}^{(0,1)}$QG's bracket (29) are given by

$$\mathcal{C}_{a,F}[\bar{\xi}, \psi_\sigma, \psi_{\sigma^2}] := \int_{\mathscr{D}} a\bar{\xi} + F(\psi_\sigma, \psi_{\sigma^2})\, d^2x \quad (41)$$

for any constant a and arbitrary function F. In Ref. [6] a proof for the $\mathrm{IL}^{(0,1)}$PE's Casimirs was given (cf. Remark 5, below). Here we present the proof for the QG case. A genuine Casimir $\mathcal{C}[\bar{\xi}, \psi_\sigma, \psi_{\sigma^2}]$ must satisfy:

$$\begin{pmatrix} \{\bar{\xi}, \cdot\}_{xy} & \{\psi_\sigma, \cdot\}_{xy} & \{\psi_{\sigma^2}, \cdot\}_{xy} \\ \{\psi_\sigma, \cdot\}_{xy} & 0 & 0 \\ \{\psi_{\sigma^2}, \cdot\}_{xy} & 0 & 0 \end{pmatrix}$$
$$\times \begin{pmatrix} \frac{\delta\mathcal{C}}{\delta\bar{\xi}} \\ \frac{\delta\mathcal{C}}{\delta\psi_\sigma} \\ \frac{\delta\mathcal{C}}{\delta\psi_{\sigma^2}} \end{pmatrix} = \begin{pmatrix} 0 \\ 0 \\ 0 \end{pmatrix}. \quad (42)$$

From the last two rows, it is clear that $\delta\mathcal{C}/\delta\bar{\xi}$ must be a constant. This makes the first term in the first row to vanish.

The last two terms vanish by adding the integral of an arbitrary function of $(\psi_\sigma, \psi_{\sigma^2})$, showing that (41) indeed is a valid Casimir. In fact, there exists no Casimir more general than (41).

Remark 5. *The admissibility conditions* (30) *are satisfied by the Casimir* $\mathcal{C}_{a,F}$, *given in* (41), *provided that* ψ_σ *and* ψ_{σ^2} *are constant along* $\partial\mathcal{D}_\pm$, *that is, provided that the coasts of the zonal channel domain* $\mathcal{D}$ *are isopycnic.* This same condition must hold in the $\mathrm{IL}^{(0,1)}\mathrm{PE}$ for its Casimirs, given by $\mathcal{C}_{a,F}[\bar{\mathbf{u}}, h, \bar{\vartheta}, \vartheta_\sigma] := \int_\mathcal{D} a\bar{q}h + F(\bar{\vartheta}, \vartheta_\sigma)\, d^2x$ f or $a =$ const and every F where $\bar{q}$ is the potential vorticity, to commute with any functional in the corresponding bracket. This Casimir family reduces to $\mathcal{C}_{a,F}$ in the QG limit.

The conservation laws above can all be verified directly. Indeed, after integrating by parts with boundary conditions (5) in mind, one computes

$$\dot{\mathcal{E}} = \bar{\psi}|_{\partial\mathcal{D}_-}\dot{\gamma}_- + \bar{\psi}|_{\partial\mathcal{D}_+}\dot{\gamma}_+, \tag{43}$$

which vanishes when the velocity circulations along the walls of the zonal channel domain are constant, justifying condition (22). As for the zonal momentum, one has that

$$\dot{\mathcal{M}} = \int_\mathcal{D} (\nabla^2\bar{\psi} - R_S^{-2}\bar{\psi} + \beta y)\partial_x\bar{\psi}\, d^2x = 0, \tag{44}$$

where the first equality follows upon cancellation of boundary terms by virtue of (5) and the second one by using (5b), in particular. In turn, verifying the constancy of $\mathcal{C}_{a,F}$ directly is a straightforward application of boundary conditions (5).

Finally, the $\mathrm{IL}^0\mathrm{QG}$ has the same motion integrals as above with R_S replaced by R in the (27) and, in particular, with (41) replaced by

$$\mathcal{C}_{F,G}[\bar{\xi}, \psi_\sigma, \psi_{\sigma^2}] := \int_\mathcal{D} \bar{\xi}F(\psi_\sigma) + G(\psi_\sigma)\, d^2x, \tag{45}$$

for arbitrary F, G, which commutes with any functional with the appropriate Lie–Poisson bracket. This Casimir is well known [4, 34]. To verify conservation of energy and zonal momentum directly one simply proceeds as above. To check conservation of (45) directly one proceeds similarly as we do to prove constancy of (46), below.

Remark 6. *In a similar manner as for the Casimir family* (41) *to be genuine, genunity of the Casimir family* (45) *imposes a condition on the boundaries of the flow's zonal channel domain: its coasts must be isopycnic.*

2.7.2. Weak Casimirs

Lemma 1. *The dynamics of the* $\mathrm{IL}^{(0,1)}QG$ *preserve the following infinite family of functionals*

$$\mathcal{I}_F[\bar{\xi}, \psi_\sigma, \psi_{\sigma^2}] := \int_\mathcal{D} \bar{\xi}F(\psi_\sigma - \tfrac{2}{3}\psi_{\sigma^2})\, d^2x, \tag{46}$$

where F *is arbitrary.*
Proof. Since $\nabla \cdot \nabla^\perp\bar{\psi} = 0$, from (4b)–(4c) one has

$$\partial_t G(\psi_\sigma, \psi_{\sigma^2}) + \nabla \cdot G(\psi_\sigma, \psi_{\sigma^2})\nabla^\perp\bar{\psi} = 0, \tag{47}$$

for every G. Integrating over $\mathcal{D}$,

$$\int_\mathcal{D} G(\psi_\sigma, \psi_{\sigma^2})\, d^2x = \text{const}, \tag{48}$$

because the flow normal to the channel walls vanishes and the there is periodicity in the along-channel direction. Now define $\chi := \psi_\sigma - (2/3)\psi_{\sigma^2}$. Multiplying (4a) by $F(\phi)$ for any F and using (47) with $G(\psi_\sigma, \psi_{\sigma^2})$ replaced by $F(\chi)$,

$$\partial_t\left(\bar{\xi}F(\chi)\right) + \nabla \cdot \bar{\xi}F(\chi)\nabla^\perp\bar{\psi} = R_S^{-2}F(\chi)\nabla \cdot \phi\nabla^\perp\bar{\psi}. \tag{49}$$

Multiplying (48) by R_S^{-2} with $G(\psi_\sigma, \psi_{\sigma^2})$ replaced by $\int F(\chi)\, d\chi$, and adding the result to (47), upon integrating over $\mathcal{D}$,

$$\int_\mathcal{D} \bar{\xi}F(\chi) + R_S^{-2}\int F(\chi)\, d\chi\, d^2x = \text{const}. \tag{50}$$

More generally, with (48) in mind,

$$\int_\mathcal{D} \bar{\xi}F(\chi) + R_S^{-2}\int F(\chi)\, d\chi$$
$$+ G(\psi_\sigma, \psi_{\sigma^2})\, d^2x = \text{const}, \tag{51}$$

from which conservation of (46) follows by choosing $G(\psi_\sigma, \psi_{\sigma^2}) = -R_S^{-2}\int F(\chi)\, d\chi$ for arbitrary F.

Three salient observations are warranted:

1. The integrals of motion (46) do *not* constitute Casimirs. Indeed,

$$\begin{pmatrix} \{\bar{\xi}, \cdot\}_{xy} & \{\psi_\sigma, \cdot\}_{xy} & \{\psi_{\sigma^2}, \cdot\}_{xy} \\ \{\psi_\sigma, \cdot\}_{xy} & 0 & 0 \\ \{\psi_{\sigma^2}, \cdot\}_{xy} & 0 & 0 \end{pmatrix}$$
$$\times \begin{pmatrix} \frac{\delta\mathcal{I}_F}{\delta\bar{\xi}} = F \\ \frac{\delta\mathcal{I}_F}{\delta\psi_\sigma} = \bar{\xi}F' \\ \frac{\delta\mathcal{I}_F}{\delta\psi_{\sigma^2}} = -\frac{2}{3}\bar{\xi}F' \end{pmatrix} = \begin{pmatrix} 0 \\ -\frac{2}{3}\{\psi_\sigma, \psi_{\sigma^2}\}_{xy}F' \\ \{\psi_{\sigma^2}, \psi_\sigma\}_{xy}F' \end{pmatrix}, \tag{52}$$

   where the last two rows in general do not vanish. That is, $\mathcal{I}_F$ does not commute with every functional in (29).

2. While conservation laws (50) and (51) are more general than $\mathcal{I}_F$, it is the first term in each case, given by $\mathcal{I}_F$, that does not represent a Casimir of the Lie–Poisson bracket (29).

3. The family of conservation laws $\mathcal{I}_F$ constitute Casimirs, but for the $\mathrm{IL}^0\mathrm{QG}$ bracket, namely,

$$\{\mathcal{F}, \mathcal{G}\}_{\bar{\xi}\chi} := \int_\mathcal{D} \bar{\xi}\left\{\frac{\delta\mathcal{F}}{\delta\bar{\xi}}, \frac{\delta\mathcal{G}}{\delta\bar{\xi}}\right\}_{xy} + \chi\left(\left\{\frac{\delta\mathcal{F}}{\delta\bar{\xi}}, \frac{\delta\mathcal{G}}{\delta\chi}\right\}_{xy}\right.$$
$$\left. + \left\{\frac{\delta\mathcal{F}}{\delta\chi}, \frac{\delta\mathcal{G}}{\delta\bar{\xi}}\right\}_{xy}\right)\, d^2x, \tag{53}$$

for all $\mathcal{F}, \mathcal{G}[\bar{\xi}, \chi]$. The IL$^{(0,1)}$QG dynamics implies the dynamics in the variables $(\bar{\xi}, \chi)$, *i.e.*, that produced by the Lie–Poisson bracket given by (53) with Hamiltonian (27), yet not *vice versa*.

The last observation above enables the interpretation of the conservation laws $\mathcal{I}_F$ as weak Casimirs as they form the kernel of the Lie-Poisson bracket for the potential vorticity evolution independent of the details of the buoyancy field as this field is advected under the flow. The connection of conservation of $\mathcal{I}_F$ with particle relabeling symmetry via Noether's theorem is discussed in Ref. [9].

Remark 7. *The IL$^{(0,1)}$PE conserves $\int_{\mathscr{D}} \bar{q} h F(\bar{\vartheta} - (1/3)\vartheta_{\sigma}) \, d^2 x$ for every F (where $\bar{q}$ is the potential vorticity). These conservation laws reduce to (46) in the low-frequency limit. The difference between the $(1/3)$ and $(2/3)$ factors is clarified upon noting that, with an $O(\mathrm{Ro}^2)$ error, $\bar{\vartheta} - g_{\mathrm{r}} - (1/3)(\vartheta_{\sigma} - (1/2)N_{\mathrm{r}}^2 H_{\mathrm{r}}) = (2g_{\mathrm{r}}/f_0 R^2)(\psi_{\sigma} - (2/3)\psi_{\sigma 2})$. The conservation laws above are not Casimirs either. However, they represent weak Casimirs in the sense previously discussed.*

3. Linear waves and free energy

Let $\varphi' := (\bar{\xi}', \psi'_{\sigma}, \psi'_{\sigma 2})$ be an infinitesimal-amplitude perturbation on

$$\Phi_{\mathrm{r}} := (-R_S^{-2}(a_1 - a_2 + \tfrac{2}{3}a_3) + \beta y, a_2, a_3), \qquad (54)$$

where a_1, a_2, a_3 are arbitrary constants. The latter represents a three-parameter family of *reference states*, i.e., stationary or equilibrium solutions of the IL$^{(0,1)}$QG system (4), subjected to (5) and (22), with *no* currents. The energy of such states, $\mathcal{E}[\Phi_{\mathrm{r}}] = [1/2]R_S^{-2}a_1^2 WL$. This identically vanishes for the particular class of reference states with $a_1 = 0$. Such a two-parameter family of reference states has the lowest possible energy and can thus be identified with the *vacuum state* [32] of the IL$^{(0,1)}$QG. The components of the perturbation field φ' evolve according to

$$\partial_t \bar{\xi}' + \beta \partial_x \bar{\psi}' = 0, \quad \partial_t \psi'_{\sigma} = 0, \quad \partial_t \psi'_{\sigma 2} = 0, \qquad (55)$$

controlling the IL$^{(0,1)}$QG linearized dynamics around (54). Assuming an (x, y, t)-dependence of the form of a normal mode, viz., $\exp \mathrm{i}(kx - \omega t) \sin ly$, satisfying the boundary conditions (5), it follows that $\psi'_{\sigma} = 0 = \psi'_{\sigma 2}$ while $\bar{\xi}' = \nabla^2 \bar{\psi}' - R_S^{-2} \bar{\psi}' \neq 0$ provided that

$$\omega = -\frac{k\beta}{k^2 + l^2 + R_S^{-2}}. \qquad (56)$$

That is, the linear waves supported by the IL$^{(0,1)}$QG are the well-known (planetary) Rossby waves [40], which do not disturb the reference buoyancy field $g_{\mathrm{r}} + (1 + (2z/H_{\mathrm{r}}))(1/2)N_{\mathrm{r}}^2 H_{\mathrm{r}}$. They correspond to the Rossby waves of the HLQG in the weak-stratification limit $S \downarrow 0$. For finite S, the (westward) phase speed is in general slower. For

instance, in the infinitely wide zonal channel case, the fastest phase speed, realized in the short-wave limit $(k, l) \downarrow (0, 0)$, is $\beta(1 - [1/3]S)R^2$, which can be up to one-third slower than that in the HLQG, given by βR^2. In addition to the Rossby waves, the IL$^{(0,1)}$QG supports an $\omega = 0$, *i.e.*, neutral, mode with $\bar{\xi}' = R_1^{-2}(\psi'_{\sigma} - [2/3]\psi'_{\sigma 2})$ with $\psi'_{\sigma}, \psi'_{\sigma 2} \neq 0$. This neutral mode is characterized by potential vorticity changes exclusively due to buoyancy changes which do not alter the fluid velocity ($\bar{\psi}' = 0$).

One test of the well-posedness of the the IL$^{(0,1)}$QG is given by the computation of the *free energy* [47]. Denoted by $\mathcal{E}_{\mathrm{free}}$, this is defined as an integral of motion quadratic to the lowest-order in the deviation from a reference state. When $\mathcal{E}_{\mathrm{free}}$ is positive definite, there cannot be a spurious growth of the amplitude of linear waves riding on the reference state as they must preserve $\mathcal{E}_{\mathrm{free}}$. A class of reference states (54) with a free energy with the desired property is defined by $(a_1/a_2) < 0$ and $(a_1/a_3) > 0$. Indeed, for such a class of reference states,

$$\mathcal{E}_{\mathrm{free}}[\bar{\xi}', \psi'_{\sigma}, \psi'_{\sigma 2}] = \mathcal{E}[\bar{\psi}'] + R_S^{-2} \int_{\mathscr{D}} \frac{2}{3}\frac{a_1}{a_3}\psi'^2_{\sigma 2}$$
$$- \frac{a_1}{a_2}\psi'^2_{\sigma} \, d^2 x, \qquad (57)$$

which is manifestly positive definite under the stated conditions. This follows by adding to the energy (27) a Casimir (41) with $a = a_1$ and $F(\psi_{\sigma}, \psi_{\sigma 2}) = R_S^{-2}((a_1/3a_3)\psi^2_{\sigma 2} - (a_1/2a_2)\psi^2_{\sigma})$. An important observation is that (57) is not restricted to infinitesimally small normal-mode perturbations. In fact, (57) is an exact integral of motion for the fully nonlinear dynamics about (54). Thus positive definiteness of (57) prevents the spurious growth of perturbations to (54) irrespective of their initial amplitude and structure.

It is fair to wonder about the dynamical significance of the constants a_1, a_2, a_3 that define the family of reference states (54) and the relationship among them for $\mathcal{E}_{\mathrm{free}}$ to be positive definite. Consider the situation in which these constants are all set to zero, in which case (54) reduces to $\Phi_{\mathrm{r}} = (\beta y, 0, 0)$, a member of the vacuum state family. The linear waves riding on this reference state are the same as those discussed above. However, in this case, the free energy can be shown to be equal to $\mathcal{E}[\bar{\psi}']$, which is positive semidefinite. Indeed, by the invertibility relationship (4d), it follows that there can be perturbations $(\bar{\xi}', \psi'_{\sigma}, \psi'_{\sigma 2})$ that do not change the free energy. Spontaneous growth of the amplitude of such perturbations cannot be constrained by free-energy conservation. An example is the neutral mode discussed above, for which the free energy identically vanishes. The same considerations apply to the complete family of vacuum states (defined by $a_1 = 0$). An important observation is that there exist Lyapunov stable states that will arrest the aforementioned spontaneous growth, should it happened, as discussed in Sec. 5, below.

Remark 8. *A result similar to that for perturbations on the vacuum state family in the IL$^{(0,1)}$QG holds for perturbations on the vacuum state in the IL$^{(0,1)}$PE parent model. In that*

model, there is a unique reference state, which is the vacuum state, and perturbations on it have a positive-semidefinite free energy associated with [47].

4. Stability of baroclinic zonal flow

Consider $\varphi := (\bar{\xi}, \psi_\sigma, \psi_{\sigma^2})$, evolving according to (4) subjected to (5) and (22). We call $\Phi := (\bar{\Xi}, \Psi_\sigma, \Psi_{\sigma^2})$ a *basic state* if it is an equilibrium of (4), subjected to (5) and (22). A particular case of basic state is the reference state discussed in Sec. 3, for which the fluid is motionless. We are interested in the stability of a basic state in the following three senses, sorted in increasing level of strength [22, 51]:

1. The first sense is *spectral stability*, in which case a perturbation $\delta\varphi(\mathbf{x}, t)$ on $\Phi(\mathbf{x})$ is assumed to be a normal mode with an infinitesimally small amplitude, viz., $\delta\varphi = \varepsilon\mathrm{Re}\{\varphi' \exp \mathrm{i}k(x - ct)\} \sin ly + O(\varepsilon^2)$ where $\varepsilon \downarrow 0$, satisfying (5) and (22). (Note the slight change of interpretation of the prime notation with respect to that used in Sec. 3.) Clearly, the amplitude of a normal mode cannot remain infinitesimally small unless $\mathrm{Im}(c) = 0$. In such a case, the basic state is said to be spectrally stable.

2. The second sense is *formal stability*. In this case $\delta\varphi$, while assumed small, can have an arbitrary structure. If there exists an integral of motion $\mathcal{H}[\varphi]$ such that $\delta\mathcal{H}[\delta\varphi; \Phi] = 0$ and $\delta^2\mathcal{H}[\delta\varphi; \Phi] > 0$, then the growth of $\delta\varphi$ will be constrained. The constraint is imposed by the quadratic nature of $\delta^2\mathcal{H}$, which is preserved by the linearized dynamics about Φ. In these circumstances one says that Φ is formally stable. Note that the free energy $\mathcal{E}_{\mathrm{free}}$ discussed in Sec. 3 is a special case of $\delta^2\mathcal{H}$ wherein Φ in motionless.

3. The third sense is *Lyapunov stability*. This relies on the possibility of proving that the total variation $\Delta\mathcal{H}[\delta\varphi; \Phi]$ is convex for finite-size $\delta\varphi$ of arbitrary structure. This means showing that $c_1\|\delta\varphi\|^2 \leq \Delta\mathcal{H} \leq c_2\|\delta\varphi\|^2$ for $c_1, c_2 = \mathrm{const}$ such that $0 < c_1 \leq c_2 < \infty$, where $\|\ \|$ is typically chosen to be an L^2 norm. Assuming that the latter holds true, since $\Delta\mathcal{H}$ is preserved under the fully nonlinear dynamics, the second inequality can be evaluated at time $t = 0$ to get $\|\delta\varphi\|_{t>0} \leq \sqrt{c_2/c_1}\|\delta\varphi\|_{t=0}$. This implies Lyapunov stability for Φ. More precisely, for every $\varrho > 0$ there exists $\varepsilon > 0$, e.g., $\varepsilon = \sqrt{(c_1/c_2)}\varrho$, such that $\|\delta\varphi\|_{t=0} < \varepsilon$ implies $\|\delta\varphi\|_{t>0} < \varrho$.

Let

$$\alpha := \frac{\bar{U}}{U_\sigma}, \quad \mu := \frac{U_{\sigma^2}}{U_\sigma}, \quad b := \frac{\beta}{U_\sigma R^2}, \quad (58\mathrm{a})$$

where $\bar{U}$, U_σ, and U_{σ^2} are constants, with the latter two required to satisfy

$$2U_\sigma - U_{\sigma^2} \geq \frac{(S - 1)f_0R^2}{2W}, \quad U_{\sigma^2} < \frac{Sf_0R^2}{4W}, \quad (58\mathrm{b})$$

by static stability; cf. (2). Our main interest is the four-parameter family of basic states defined by

$$\bar{\Psi} = -\bar{U}y, \quad \Psi_\sigma = -U_\sigma y, \quad \Psi_{\sigma^2} = -U_{\sigma^2}y, \quad (58\mathrm{c})$$

implying

$$\bar{\Xi} = -R_S^{-2}\bar{\Psi} + R_S^{-2}\left(\Psi_\sigma - \tfrac{2}{3}\Psi_{\sigma^2}\right) + \beta y = R_S^{-2}\nu\Psi_\sigma = R_S^{-2}\mu^{-1}\nu\Psi_{\sigma^2}, \quad (58\mathrm{d})$$

where

$$\nu(S) := 1 + \alpha + s(S)b - \tfrac{2}{3}\mu,$$
$$s(S) := R_S^2 R^{-2} = 1 - \tfrac{1}{3}S, \quad (58\mathrm{e})$$

which we introduce to simplify algebraic expressions below. By the thermal-wind balance, (58) implicitly corresponds, for parameters fixed, to a meridionally uniform zonal current with quadratic vertical shear, *i.e.*, a baroclinic flow with *vertical curvature* on the β-plane. Nondimensional parameters α and μ thus measure the vertical linear shear and curvature of the jet, respectively. But, by virtue of (9)–(11), one also has that

$$\alpha = 1 + \frac{2sg_\mathrm{r}}{H_\mathrm{r}} \frac{H'(y)}{\bar{\Theta}'(y)} - \frac{H_\mathrm{r}}{6} \frac{(N^2)'(y)}{\bar{\Theta}'(y)},$$
$$\mu = \frac{H_\mathrm{r}}{4} \frac{(N^2)'(y)}{\bar{\Theta}'(y)}, \quad (59)$$

where H is the layer thickness in the basic state, $\bar{\Theta}$ is the basic vertically averaged buoyancy, and $N^2 = 2\Theta_\sigma/H_\mathrm{r}$ is the basic state buoyancy frequency squared. This enables further physical insight into the (spectral) stability problem. Finally, nondimensional parameter b measures the strength of the β effect, which can be identified with a Charney number.

4.1. Spectral stability

Let

$$\lambda := \frac{c - \bar{U}}{U_\sigma}, \qquad \kappa := R\sqrt{k^2 + l^2}, \quad (60)$$

representing normalized Doppler shifted phase speed and wavenumber $\mathbf{k} = (k, l)$ (with k pointing eastward and l northward) magnitude, respectively. The following eigenvalue problem follows upon proposing a normal-mode perturbation on (58):

$$\begin{pmatrix} (s\kappa^2+1)\,\lambda+\alpha+sb & -(\lambda+\alpha) & \tfrac{2}{3}(\lambda+\alpha) \\ -1 & -\lambda & 0 \\ v\mu & 0 & -\lambda \end{pmatrix} \begin{pmatrix} \bar{\psi}' \\ \psi'_\sigma \\ \psi'_{\sigma^2} \end{pmatrix} = 0. \quad (61)$$

Nontrivial solutions exist provided that the determinant of the matrix of the eigenproblem vanishes. This leads to the dispersion relation

$$\lambda = \frac{-\nu \pm \sqrt{\nu^2 - 4\alpha\left(1 - \frac{2}{3}\mu\right)\left(s\kappa^2 + 1\right)}}{2\left(s\kappa^2 + 1\right)}. \tag{62}$$

Spectral stability is realized when the perturbation phase speed c, or equivalently λ, is real. A sufficient condition for this is

$$\alpha\left(1 - \frac{2}{3}\mu\right) < 0. \tag{63}$$

The shaded quadrants in Fig. 3 are subsets of the region in the (α, μ)-space defined by (63), namely,
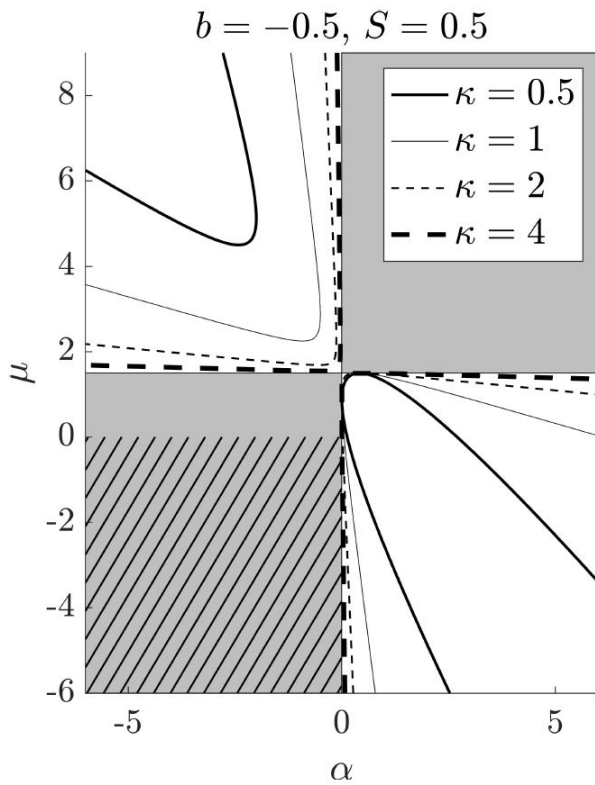

FIGURE 3. Stability of the basic state family (58), representing baroclinic zonal jets, in the $\alpha := \bar{U}/U_\sigma$ vs $\mu := U_{\sigma^2}/U_\sigma$ space, respectively measuring the vertical linear shear and curvature of a jet in the family. In the shaded regions, corresponding to the set $\mathbb{S}$ defined by $\alpha(1 - (2/3)\mu) \le 0$, the phase speed of an infinitesimally-small normal-mode perturbation is real for every wavenumber. Within the hatched region, the subset $\mathbb{L} := \{\mu < 0\} \cap \{\alpha < 0\}$ of $\mathbb{S}$, there is stability for finite-size perturbations of arbitrary structure. Moreover, in $\mathbb{L}$ the distance, in an L^2 sense, of a perturbation to the basic state is at all times bounded by a multiple of its initial distance. This means that in $\mathbb{L}$ there is Lyapunov stability. Spectral stability is possible inside the white regions, the complement of $\mathbb{S}$, $\mathbb{S}^c$. The curves labeled by the normalized wavenumber magnitude $\kappa := R\sqrt{k^2 + l^2}$ bound the (α, μ)-subregions of $\mathbb{S}^c$ where there is spectral instability for the normalized β and stratification parameters, $b := \beta/U_\sigma R^2$ and $S := N_r^2 H_r/2g_r$, respectively, as indicated.

$$\{\alpha < 0\} \cap \{\mu < \tfrac{3}{2}\} \bigcup \{\alpha > 0\} \cap \{\mu > \tfrac{3}{2}\}, \tag{64}$$

where there is spectral stability of basic state (58) for every wavenumber. *This holds independent of the values taken by the Charney number (b) and stratification parameter (S).* By virtue of (59), one concludes that the basic states in the upper-right (resp., lower-left) clear quadrant have $H'(y)$ and $\bar{\Theta}'(y)$ with like (resp., opposing) signs and $\bar{\Theta}'(y)/(N^2)'(y)$ smaller (resp., larger) than $(1/6)H_r$. The curves labeled by κ bound the (sub)regions of the (α, μ)-plane where there is spectral instability, *i.e.*, (63) is violated, for selected b and S values. Note the asymmetry, with less basic states being spectrally unstable toward smaller wavenumbers in the region $\{\alpha < 0\} \cap \{\mu > (3/2)\}$ than in the region $\{\alpha > 0\} \cap \{\mu < (3/2)\}$. This behavior reverses with positive values of b.

More specifically, in the limit $\kappa \downarrow 0$, (66) equals

$$\lambda = -\tfrac{1}{2}\nu \pm \tfrac{1}{2}\sqrt{\nu^2 - 4\alpha\left(1 - \tfrac{2}{3}\mu\right)}, \tag{65}$$

which is complex where $\alpha(1 - (2/3)\mu) > (1/4)\nu^2 = (1/4)\left(1 + \alpha + sb - (2/3)\mu\right)^2$ (and real otherwise, making explicit that (63) is sufficient, yet not necessary, for spectral stability). At criticality, one finds that $\mu = (2/3)(1 - \alpha + sb) \pm (3/2)\sqrt{(1 - \alpha + sb) - (1 + \alpha + sb)^2 + 4\alpha}$. This represents a parabola with tangencies on the curve $C_+ := \{\alpha = 0, \mu > (3/2)\} \cup \{\alpha > 0, \mu = (3/2)\}$, when $b < 0$, and the curve $C_- := \{\alpha = 0, \mu < (3/2)\} \cup \{\alpha < 0, \mu = (3/2)\}$, when $b > 0$, making more explicit the asymmetry noted above. For completeness, we note that in the limit $\kappa \uparrow \infty$ there is spectral stability everywhere in the (α, μ)-space where (63) is violated, in such a case for any b and S. Indeed,

$$\lambda \sim \pm i\sqrt{\frac{\alpha(1 - \frac{2}{3}\mu)}{1 - \frac{1}{3}S}}\kappa^{-1} \tag{66}$$

asymptotically as $\kappa \uparrow \infty$. The curves $\kappa \uparrow \infty$ in the (α, μ)-plane are given by $C_\pm$. Their union $\{\alpha = 0, \mu = (3/2)\}$ corresponds to the set of basic states lying at the boundary of spectral stability. Thus, unlike all other curves in the spectrally unstable regions of the (α, μ)-plane, the curves $C_\pm$ do not bound spectrally unstable states.

In Fig. 4 we depict dispersion relation (62) as a function of the wavenumber, more precisely c/U_σ vs κ, for selected values of the various basic state parameters. The onset of instability happens at the wavenumber where the two branches of the dispersion relation merge. Included in the plot for reference is the asymptotic expression for c/U_σ as $\kappa \uparrow \infty$, as it follows from (66). Also indicated is $\lim_{\kappa\uparrow\infty} c/U_\sigma = \alpha$, that is, a real number, irrespective of the parameters that define the basic state.
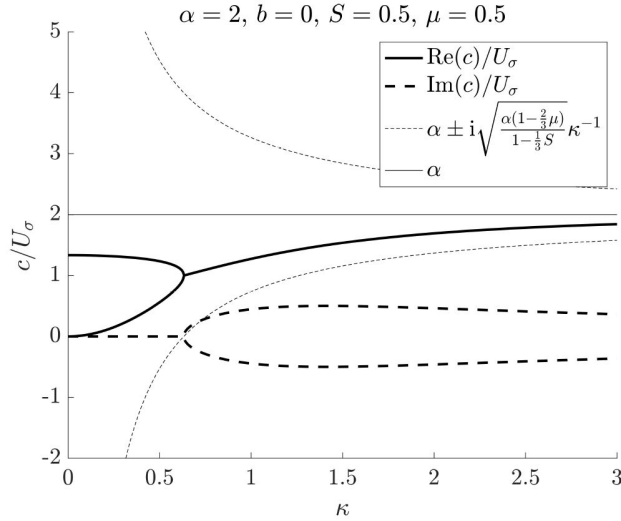
FIGURE 4. As a function of normalized wavenumber, normalized phase speed for a normal-mode perturbation on the baroclinic zonal jet defined by (58) with parameters as indicated. Asymptotic dispersion relation curves as $\kappa \uparrow \infty$ and the corresponding limiting value are included.

In the limit of weak stratification, *i.e.*, $S \downarrow 0$, the length scales R and $L := N_r H_r / |f_0|$ are well separated. The latter is proportional to the gravest baroclinic (internal) Rossby radius of deformation in a model with arbitrary stratification.

Since we are assuming a reduced-gravity setting, R and L can be approximately identified with the first and second internal deformation radii, respectively, of the arbitrarily stratified model extending throughout the entire water column. The noted scale separation allows one to distinguish long perturbations, with wavenumbers $\kappa = O(1)$ as $S \downarrow 0$, from short perturbations, with wavenumbers $L|\mathbf{k}| = \sqrt{2S}\kappa = O(1)$ as $S \downarrow 0$. We find that (62) reduces to

$$\lambda = \frac{-\nu(0) \pm \sqrt{\nu(0)^2 - 4\alpha \left(1 - \frac{2}{3}\mu\right)\left(\kappa^2 + 1\right)}}{2\left(\kappa^2 + 1\right)}, \quad (67)$$

for long perturbations, and $\lambda = 0$, for short perturbations. The limit $\kappa \uparrow \infty$ of (67) gives $\lambda = 0$, *i.e.*, $c = \bar{U}$. As expected, it coincides with the short-perturbation phase speed. This is real for all wavenumbers, which can be anticipated to be consequential for direct, fully nonlinear simulations. It seems reasonable to think that wave activity in such simulations will fall off at sufficiently large wavenumbers (short wavelengths), which, according to the spectral (*i.e.*, linear) analysis, are not growing.

Concerning the growth rate of the perturbation, given by $\varpi := k\,\mathrm{Im}(c)$ for the smallest meridional wavenumber, viz., $l = \pi/W$, it is observed that this saturates with zonal wavenumber, both when the stratification is finite and for long perturbations in the weak-stratification limit. The left panel of Fig. 5 shows $\varpi(k)$ when $W = R$ for selected values of basic state parameters outside the spectrally stable set (64) in the limit of weak stratification and with vanishing Charney number. Note that ϖ is larger (resp., smaller) when the basic state zonal velocity vertical profile (Fig. 5, middle panel) curves eastward (resp., westward) than when it does not curve, as in the IL^{0}QG. An upper-bound measure of the saturating value of ϖ is given, when S is finite, by

$$\max_{\kappa} \frac{\kappa\,\mathrm{Im}(c)}{U_\sigma} = \sqrt{\frac{\alpha\left(1 - \frac{2}{3}\mu\right)}{1 - \frac{1}{3}S}}, \quad (68)$$

where parameters (α, μ) belong in the spectrally unstable region, *i.e.*, the complement of set (64). The long-perturbation limit of (68) is $\sqrt{\alpha(1 - (2/3)\mu)}$, which we plot in right panel of Fig. 5. An important final observation, with consequences for direct simulations, is that the growth rate for short perturbations vanishes for all wavenumbers, reinforcing the comments above that development of wave activity should be stopped in the IL$^{(0,1)}$QG at sufficiently short wavelengths.
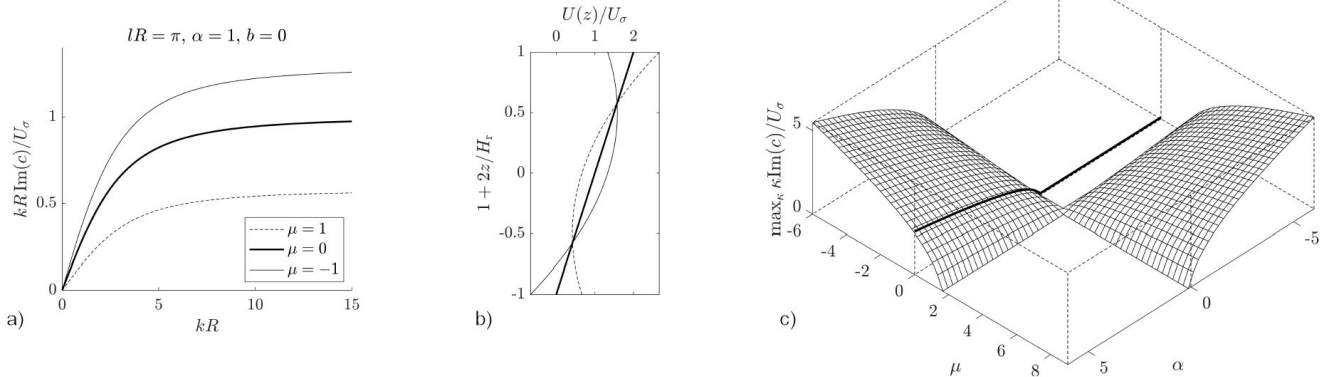

FIGURE 5. a) Growth rate as a function of zonal wavenumber in the limit of weak stratification ($S \downarrow 0$) with basic state parameters α and b as indicated for three values of μ. The IL^{0}QG result corresponds to the $\mu = 0$ curve as the velocity in that model can only include linear shear (implicitly, by the thermal-wind balance). b) Zonal velocity (implicit) vertical profiles leading to the growth rates in the left panel. c) Upper bound on the growth rate in (α, μ)-space for weak stratification. The thick line is the corresponding result for the IL^{0}Q.

4.2. Formal stability

We now turn to investigate the formal stability of basic satate (58), for which we have at our disposal several conservation laws, namely, energy ($\mathcal{E}$), Casimirs ($\mathcal{C}_{a,F}$), zonal momentum ($\mathcal{M}$), and the non-Casimir, non-explicit-symmetry-related conservation laws ($\mathcal{I}_F$) (cf. Sec. 2.7) to construct an appropriate general integral of motion $\mathcal{H}$ such that $\delta\mathcal{H} = 0$ at a basic state. The use of energy and Casimirs to construct $\mathcal{H}$ may be traced from the work of Arnold in the 1960's [which is a collection of papers that appeared in those years] [2] back over a decade to those of [15, 25]. The use of momentum in systems with x-translational symmetry was pioneered by Ripa [43]. Here we explore the additional use of the weak Casimir conservation law $\mathcal{I}_F$. We these comments in mind, we will, following tradition, refer to the use of all available integrals of motion to derive a-priori stability statements as *Arnold's method*.

Remark 9. *A few remarks are in order:*

1. The equilibria Φ of a Hamiltonian system $\partial_t\varphi = \{\varphi, \mathcal{E}\}$ are no longer unrestricted conditional extrema of the Hamiltonian ($\mathcal{E}$); by contrast, $\partial_t\Phi = \{\Phi, \mathcal{E}[\Phi]\}[\Phi] = 0$ implies that $(\delta/\delta\varphi)(\mathcal{E} + \mathcal{C})[\Phi] = 0$ for some Casimir $\mathcal{C}$. Level sets of constants of the motion define certain "leaves" on the Poisson manifold, $(P, \{ , \})$. If these constants are the Casimirs of $\{ , \}$, they form the "symplectic leaves" of P [22, 36]. Thus equilibria (basic states) are critical "points" of $\mathcal{E}$ restricted to such leaves.

2. When $\mathcal{H}$ is chosen to be a linear combination $\mathcal{E} + \mathcal{C} - U\mathcal{M}$ where $U = \mathrm{const}$ and for some $\mathcal{C}$ such that $\delta\mathcal{H} = 0$ at Φ, it turns out that $\delta^2\mathcal{H}$ is a Hamiltonian for the linearized dynamics about Φ as seen from a reference frame steadily translating in the x-direction with speed U. Namely, to the lowest order in $\delta\varphi$, it follows that $(\partial_t + U\partial_x)\delta\varphi = \{\delta\varphi, \delta^2\mathcal{H}\}[\Phi]$ where the bracket here is that defined in Eq. (29) but with a constant argument. This is a genuine Lie–Poisson bracket in that all required properties are satisfied, most importantly the Jacobi identity, which is readily verified cf., [for a discussion] [32].

3. With $\mathcal{H}$ as constructed, the integral $\delta^2\mathcal{H}$, or more generally $\Delta\mathcal{H}$, is referred to as **pseudoenergy–momentum**, following notation introduced in Ref. [43]. In the case with no zonal symmetry, the *pseudoenergy* is referred to as a "free energy" in Ref. [36] to mean that it is the energy accessible to the system upon perturbation away from equilibrium given the Casimir. It should not be confused with the free energy defined in Sec. 3.

We begin by considering

$$\mathcal{H}_{\bar{U}} := \mathcal{E} - \bar{U}\mathcal{M} + \mathcal{C}_{0,F}, \qquad (69)$$

with

$$F(\psi_\sigma, \psi_{\sigma^2}) = -\tfrac{1}{2}\alpha R_S^{-2}\left(\psi_\sigma^2 - \tfrac{2}{3}\mu^{-1}\psi_{\sigma^2}^2\right). \qquad (70)$$

The first variation of (69) identically vanishes at the basic state (58). Its second variation

$$\delta^2\mathcal{H}_{\bar{U}} = \mathcal{E}[\delta\bar{\psi}] - \tfrac{1}{2}R_S^{-2}\alpha\int\delta\psi_\sigma^2 - \tfrac{2}{3}\mu^{-1}\delta\psi_{\sigma^2}^2\, d^2x, \quad (71)$$

which is positive definite provided that

$$\alpha < 0, \quad \mu < 0. \qquad (72)$$

This corresponds to the hatched region of the (α, μ)-plane of Fig. 3. That is, only a subset of the spectrally stable states are possible to be proved formally stable. But such a subset however is stable with respect to perturbations not only of arbitrary structure. Rather, they are stable with respect to finite-amplitude perturbations since

$$\delta^2\mathcal{H}_{\bar{U}} = \Delta\mathcal{H}_{\bar{U}}. \qquad (73)$$

That is, the pseudoenergy–momentum is a quadratic integral of motion. This is a Hamiltonian for the exact dynamics of the IL$^{(0,1)}$ as seen by an observer zonally moving with speed $\bar{U}$ (extending Remark 9(ii), above). We will return to discussing the consequences of (73) in Sec. 4.3, below.

Let us consider now the use of the weak Casimir integrals $\mathcal{I}_F$, defined in (46), in Arnold's method. It turns out that the general integral of motion

$$\mathcal{H}_{\frac{2}{3}\alpha U_\sigma} := \mathcal{E} - \tfrac{2}{3}\alpha U_\sigma\mathcal{M} + \mathcal{C}_{0,F} + \mathcal{I}_G. \qquad (74)$$

for

$$F(\psi_\sigma, \psi_{\sigma^2}) = \tfrac{1}{2}R_S^{-2}\alpha(\nu + 1)\left(\tfrac{2}{3}\nu^{-1}\psi_{\sigma^2}^2 - \psi_\sigma^2\right), \quad (75)$$

$$G\left(\psi_\sigma - \tfrac{2}{3}\psi_{\sigma^2}\right) = \alpha\left(\psi_\sigma - \tfrac{2}{3}\psi_{\sigma^2}\right), \qquad (76)$$

has a vanishing first variation at the basic state (58). Its second variation,

$$\delta^2\mathcal{H}_{\frac{2}{3}\alpha U_\sigma} = \mathcal{E}[\delta\bar{\psi}] + \alpha\int\left(\delta\bar{\xi} + \tfrac{1}{2}\delta\psi_\sigma\right)^2 - \left(\delta\bar{\xi} + \tfrac{1}{3}\delta\psi_{\sigma^2}\right)^2$$
$$- \tfrac{1}{2}\left(R_S^{-2}(\nu + 1) + \tfrac{1}{2}\right)\delta\psi_\sigma^2$$
$$+ \tfrac{1}{3}\left(R_S^{-2}\mu^{-1}(\nu + 1) - \tfrac{1}{3}\right)\delta\psi_{\sigma^2}^2\, d^2x. \qquad (77)$$

Higher-order variations of (74) vanish, so (77) is an exact, fully nonlinear conservation law. However, it is at most positive semidefinite and provided that $\alpha = 0$. Thus the conservation laws (46) are not useful to make an *a priori* assessment about the stability of the basic state (58), at least using Arnold's method.

4.3. Lyapunov stability

Lyapunov stability of the basic states defined by (72) can be established as follows. Consider the subset of stable basic states with

$$\alpha < 0, \quad 0 > \mu \geq -1. \tag{78}$$

Let η_1 and λ_1 be two positive constants such that

$$0 < \eta_1 < -\alpha, \tag{79}$$

and

$$-\alpha - \eta_1 \leq \lambda_1 \leq -\alpha + \eta_1, \tag{80}$$

respectively. Recalling that (73) holds, the convexity estimate follows:

$$\frac{-\alpha - \eta_1}{\lambda_1} \|(\delta\bar{\xi}, \delta\psi_\sigma, \delta\psi_{\sigma^2})\|_2(\lambda_1)^2 \leq \Delta\mathcal{H}_{\bar{U}}$$
$$\leq \frac{-\alpha + \eta_1}{\lambda_1} \|(\delta\bar{\xi}, \delta\psi_\sigma, \delta\psi_{\sigma^2})\|_2(\lambda_1)^2, \tag{81}$$

where

$$\|(\delta\bar{\xi}, \delta\psi_\sigma, \delta\psi_{\sigma^2})\|_2(\lambda_1)^2 := \mathcal{E}[\delta\bar{\psi}] + \tfrac{1}{2}R_S^{-2}\lambda_1 \int \delta\psi_\sigma^2$$
$$+ \tfrac{2}{3}\delta\psi_{\sigma^2}^2 \, d^2x, \tag{82}$$

measures, in an L^2 sense, the squared distance to the subfamily of basic states (58) defined by (78) in the infinite-dimensional phase space of the $\mathrm{IL}^{(0,1)}\mathrm{QG}$ model Eq. (4) with coordinates $(\bar{\xi}, \psi_\sigma, \psi_{\sigma^2})$. This establishes Lyapunov stability for them. Indeed, since $\Delta\mathcal{H}_{\bar{U}}$ is invariant and convex, it follows that the distance to such states at any time is bounded from above by a multiple of the initial distance.

Consider now the subfamily of basic states (58) defined by

$$\alpha < 0, \quad \mu < -1. \tag{83}$$

Letting η_2 and λ_2 be positive constants such that

$$0 < \eta_2 < \frac{\alpha}{\mu}, \tag{84}$$

and

$$\frac{\alpha}{\mu} - \eta_2 \leq \lambda_2 \leq \frac{\alpha}{\mu} + \eta_2, \tag{85}$$

one finds the convexity estimate:

$$\frac{\alpha - \mu\eta_2}{\mu\lambda_2} \|(\delta\bar{\xi}, \delta\psi_\sigma, \delta\psi_{\sigma^2})\|_2(\lambda_2)^2 \leq \Delta\mathcal{H}_{\bar{U}} \leq \frac{\alpha + \mu\eta_1}{\mu\lambda_2}$$
$$\times \|(\delta\bar{\xi}, \delta\psi_\sigma, \delta\psi_{\sigma^2})\|_2(\lambda_2)^2. \tag{86}$$

This establishes Lyapunov stability for basic states (58) with (83). Overall the above convexity estimates establish Lyapunov stability for (58) over the whole range of stable parameters (72).

5. Nonlinear saturation of unstable baroclinic zonal flow

In this section we seek to a-prior constraining the growth of perturbations to basic states (58) that have been found to be spectrally unstable, namely, those that violate (63), by making use of the above Lyapunov stability result(s) for basic states (58) satisfying (72). This can be done using *Shepherd's method*, introduced in Ref. [53], which we outline below. Denote stable (resp., unstable) state quantities with a superscript S (resp., U). Grouping $(\bar{\xi}, \psi_\sigma, \psi_{\sigma^2})$ into φ we have

$$\|\varphi - \Phi^{\mathrm{U}}\|_2(\lambda_1) \leq \sqrt{\frac{2\alpha^{\mathrm{S}}}{\alpha^{\mathrm{S}} + \eta_1}}$$
$$\times \|\Phi^{\mathrm{S}} - \Phi^{\mathrm{U}}\|_2(\lambda_1) =: \mathcal{B}_1, \tag{87}$$

for Φ^{S} satisfying (78) and

$$\|\varphi - \Phi^{\mathrm{U}}\|_2(\lambda_2) \leq \sqrt{\frac{2\alpha^{\mathrm{S}}}{\alpha^{\mathrm{S}} - \mu^{\mathrm{S}}\eta_2}}$$
$$\times \|\Phi^{\mathrm{S}} - \Phi^{\mathrm{U}}\|_2(\lambda_2) =: \mathcal{B}_2, \tag{88}$$

for Φ^{S} satisfying (83). The inequalities above follow as a result of successively:

1. applying the triangular inequality $\|\varphi - \Phi^{\mathrm{U}}\|_2(\lambda_i) \leq \|\varphi - \Phi^{\mathrm{S}}\|_2(\lambda_i) + \|\Phi^{\mathrm{S}} - \Phi^{\mathrm{U}}\|_2(\lambda_i), i = 1, 2$;

2. using convexity estimate (81) for $i = 1$ and (86) for $i = 2$; and

3. *assuming that $\varphi \approx \Phi^{\mathrm{U}}$ initially at $t = 0$.*

Set λ_1 and λ_2 to their minimum values in their corresponding admissible ranges, given by (80) and (85), respectively. Let

$$0 < r_i < 1, \quad i = 1, 2, \tag{89}$$

be constants such that

$$\eta_1 = -r_1\alpha^{\mathrm{S}}, \quad \eta_2 = r_2\frac{\alpha^{\mathrm{S}}}{\mu^{\mathrm{S}}}, \tag{90}$$

satisfy (79) and (84), respectively. The following tighter bounds result upon minimizing over r_i, $i = 1, 2$:
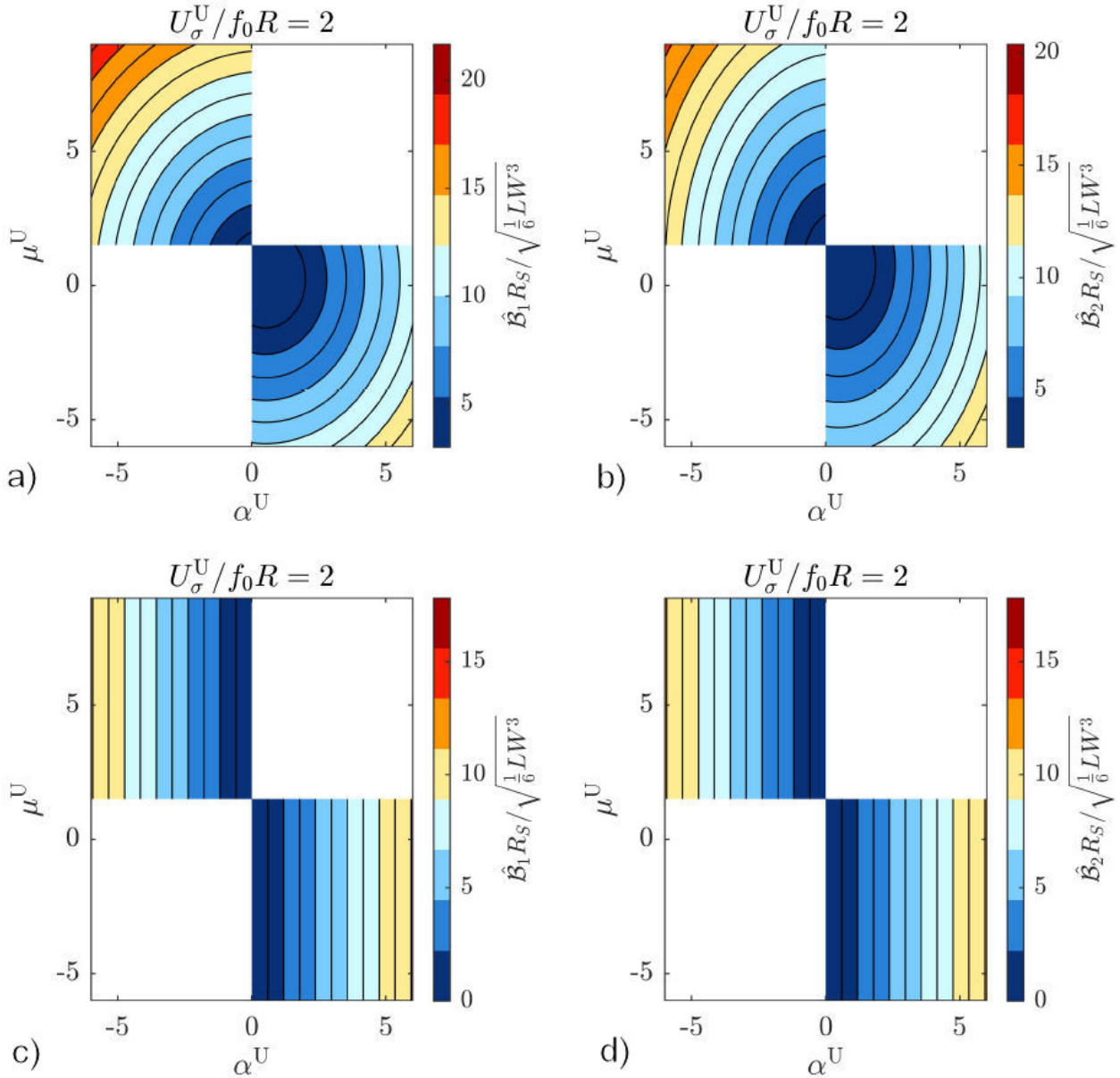
FIGURE 6. Normalized a-priori nonlinear upper bounds on the growth of perturbations to spectrally unstable basic states as computed using Lyapunov-stable states with $\alpha^S < 0$ and $0 > \mu^S \geq -1$ a) and $\alpha^S < 0$ and $\mu^S < -1$ b). The bottom panels show the same as in the top panels in the limit $\bar{U}^S \downarrow 0$.

$$\mathcal{B}_1 \geq \hat{\mathcal{B}}_1 := R_S^{-1}\sqrt{\tfrac{1}{6}LW^3} \cdot \sqrt{(\bar{U}^S - \bar{U}^U)^2 - \frac{\bar{U}^S}{U_\sigma^S}\left((U_\sigma^S - U_\sigma^U)^2 + \tfrac{2}{3}(U_{\sigma^2}^S - U_{\sigma^2}^U)^2\right)}, \tag{91}$$

and

$$\mathcal{B}_2 \geq \hat{\mathcal{B}}_2 := R_S^{-1}\sqrt{\tfrac{1}{6}LW^3} \cdot \sqrt{(\bar{U}^S - \bar{U}^U)^2 + \frac{\bar{U}^S}{U_{\sigma^2}^S}\left((U_\sigma^S - U_\sigma^U)^2 + \tfrac{2}{3}(U_{\sigma^2}^S - U_{\sigma^2}^U)^2\right)}. \tag{92}$$

In the upper-left panel of Fig. 6, we illustrate $\hat{\mathcal{B}}_1$ within the (α^U, μ^U)-space for $U_\sigma^U = 2f_0R$, calculated utilizing $\bar{U}^S = f_0R$, $U_\sigma^S = -f_0R$, and $U_{\sigma^2}^S = (1/2)f_0R$. Similarly, the upper-right panel of Fig. 6 depicts $\hat{\mathcal{B}}_2$, derived using $\bar{U}^S = f_0R$, $U_\sigma^S = -f_0R$, and $U_{\sigma^2}^S = (3/2)f_0R$. It is important to note that at the boundary of instability, these bounds do not reach zero. They indeed approach zero along $\alpha^U = 0$ as $\bar{U}^S \downarrow 0$ (Fig. 6, bottom panels), but not along $\mu^U = 3/2$, since the Lyapunov-stable basic states only cover a portion of the complement to the spectrally stable zone in the (α, μ)-space (cf. Fig. 3). Optimal bounds can

be found by minimizing $\hat{\mathcal{B}}_1$ and $\hat{\mathcal{B}}_2$ over stable state parameters. The key point is the presence of a-priori upper bounds that restrict disturbances to spectrally unstable basic states, specifically equilibria (58) that violate (63), from experiencing an ultraviolet blowup.

Finally, following the findings presented in Ref. [8], Shepherd's method serves as a means to constrain the growth of perturbations on unstable states that may pertain to a distinct class from those for which Lyapunov stability is established. Consequently, this inference extends to perturbed vacuum states, which are characterized by positive-semidefinite free energy (cf. Sec. 3), representing a variant of pseudo-energy–momentum. Essentially, their nonlinear growth is restricted by the presence of Lyapunov-stable basic states, similar to the nonlinear growth of perturbations to unstable basic states with sign-indefinite pseudo-energy–momentum. The constraints on the potential spontaneous growth of perturbations to the vacuum state, if it occurs, are given by either (91) or (92) with $\bar{U}^{\mathrm{U}} = U_\sigma^{\mathrm{U}} = U_{\sigma^2}^{\mathrm{U}} = 0$.

6. Discussion

The study presented here was motivated, in part, by direct numerical simulations revealing a tendency of the $\mathrm{IL}^0\mathrm{QG}$ to quickly develop visually more intense small-scale vortex rolls than the $\mathrm{IL}^{(0,1)}\mathrm{QG}$ [6]. Such small-scale circulation can be fairly referred to as submsoscales circulations as their scales fall well below R, the Rossby deformation radius in the $\mathrm{IL}^0\mathrm{QG}$ and $\mathrm{IL}^{(0,1)}\mathrm{QG}$ models. As noted above, being R an equivalent barotropic deformation radius, it approximately corresponds to the gravest baroclinic (*i.e.*, internal) deformation scale in the continuously stratified model defined over the entire water column. The results from the various analyses carried out above do not appear to provide reason to expect that the numerical observation of [6] holds in general, as we summarize next:

1. The production (or destruction) of Kelvin–Noether circulation ($\mathcal{K}$) along material loops was identified in [20] with the development of sub-deformation scale or submesoscale wave activity in the $\mathrm{IL}^0\mathrm{QG}$. It turns out that $\mathcal{K}$ is equally produced (or destroyed) in both the $\mathrm{IL}^0\mathrm{QG}$ and $\mathrm{IL}^{(0,1)}\mathrm{QG}$. The rate of change of $\mathcal{K}$ in the former is given by (19) with the $-2/3\psi_{\sigma^2}$ term omitted. While by static stability one has that $-2/3\psi_{\sigma^2} < 1/6 f_0 R^2 S$, one cannot anticipate the contribution of the gradient of this term to the integral in Eq. (19). In other words, one cannot anticipate the role of stratification in the production (or destruction) of $\mathcal{K}$.

2. Both the $\mathrm{IL}^0\mathrm{QG}$ and $\mathrm{IL}^{(0,1)}\mathrm{QG}$ models exhibit a neutral mode, termed a "force compensating mode" by [48], where potential vorticity changes arising from buoyancy fluctuations do not alter the fluid velocity (cf. Sec. 3). That is, associated with this mode is a vanishing free energy, which cannot constrain a possible spontaneous growth of this mode. Thus, both the

$\mathrm{IL}^0\mathrm{QG}$ and $\mathrm{IL}^{(0,1)}\mathrm{QG}$ suffer from this property, which might equally play a role in the development of submesoscale circulations in both models.

3. The intensity of submesoscale motions is constrained by the existence of Lyapunov-stable states, both in the $\mathrm{IL}^{(0,1)}\mathrm{QG}$ (cf. Sec. 5) and the $\mathrm{IL}^0\mathrm{QG}$ [8]. However, one cannot compare the size of the space available in each model for wave activity, more precisely, the nonlinear growth of the amplitude of perturbations on basic states (58) violating (63), the condition for spectral stability. The reason is that this is measured using different (L^2) norms.

4. When considering stability itself, it was found that this predicts growth rates in the $\mathrm{IL}^{(0,1)}\mathrm{QG}$ that can be smaller than, equal to, or larger than those in the $\mathrm{IL}^0\mathrm{QG}$ (cf., *e.g.*, Fig. 5). The only, potentially important, difference is that the growth rate vanishes in the $\mathrm{IL}^{(0,1)}\mathrm{QG}$ for short perturbations. Distinguishing short from large perturbations in the weak stratification limit is only possible in $\mathrm{IL}^{(0,1)}\mathrm{QG}$.

5. Yet, that Arnold's method fails to demonstrate formal, let alone Lyapunov, stability for all spectrally stable states (cf. Fig. 3) suggests that the $\mathrm{IL}^{(0,1)}\mathrm{QG}$ may be more prone to instability than the $\mathrm{IL}^0\mathrm{QG}$, in which case all spectrally stable basic states (in a similar class) are provable Lyapunov stable [8,9].

We back up the above inferences with the results from direct numerical simulations (cf. Appendix for numerical details) of the $\mathrm{IL}^{(0,1)}$ and $\mathrm{IL}^0\mathrm{QG}$. These differ from those of [6], which included Hamiltoninan topographic forcing (cf. Sec. 2.6). Concretely, we considered the full nonlinear evolution of perturbations to the spectrally unstable basic state (58) defined by $\alpha = 3$, $\mu = 0$, $b = 0$, and $S = 0$, which violates (63). The initial perturbation was chosen to be a small-amplitude normal mode. Taking the zonal channel domain period (L) and width (W) to be equal to the deformation radius (R), the initial perturbation reads

$$\frac{R\delta\bar{\xi}}{U_\sigma} = -\frac{\delta\psi_\sigma}{RU_\sigma} = \frac{\delta\psi_{\sigma^2}}{RU_\sigma} = \frac{1}{2}\cos 4\pi\frac{x}{R}\sin\pi\frac{y}{R}. \quad (93)$$

For wavenumber-(2,1) $\mathbf{k} = (k,l) = (4\pi/R, \pi/R)$ and the above basic state parameters, from dispersion relation (62) we compute a growth rate of $\varpi \approx 1.7(U_\sigma/R)$ for the initial perturbation. The duration of the simulation was set to roughly $5\varpi^{-1}$, that is, five times the e-folding time of a growing normal mode. Snapshots of perturbation potential vorticity, $\delta\bar{\xi}$, at $t = 2.5\varpi^{-1}$ and $5\varpi^{-1}$ are shown in the top- and bottom-left panel of Fig. 7, respectively. Note the development of Kelvin–Helmholtz-like vortex rolls with scales much smaller than R. Initially, a scale separation is very evident. This evidence faints with time. The right panels of Fig. 7 show at corresponding times $\delta\bar{\xi}$ but in the $\mathrm{IL}^0\mathrm{QG}$. This was
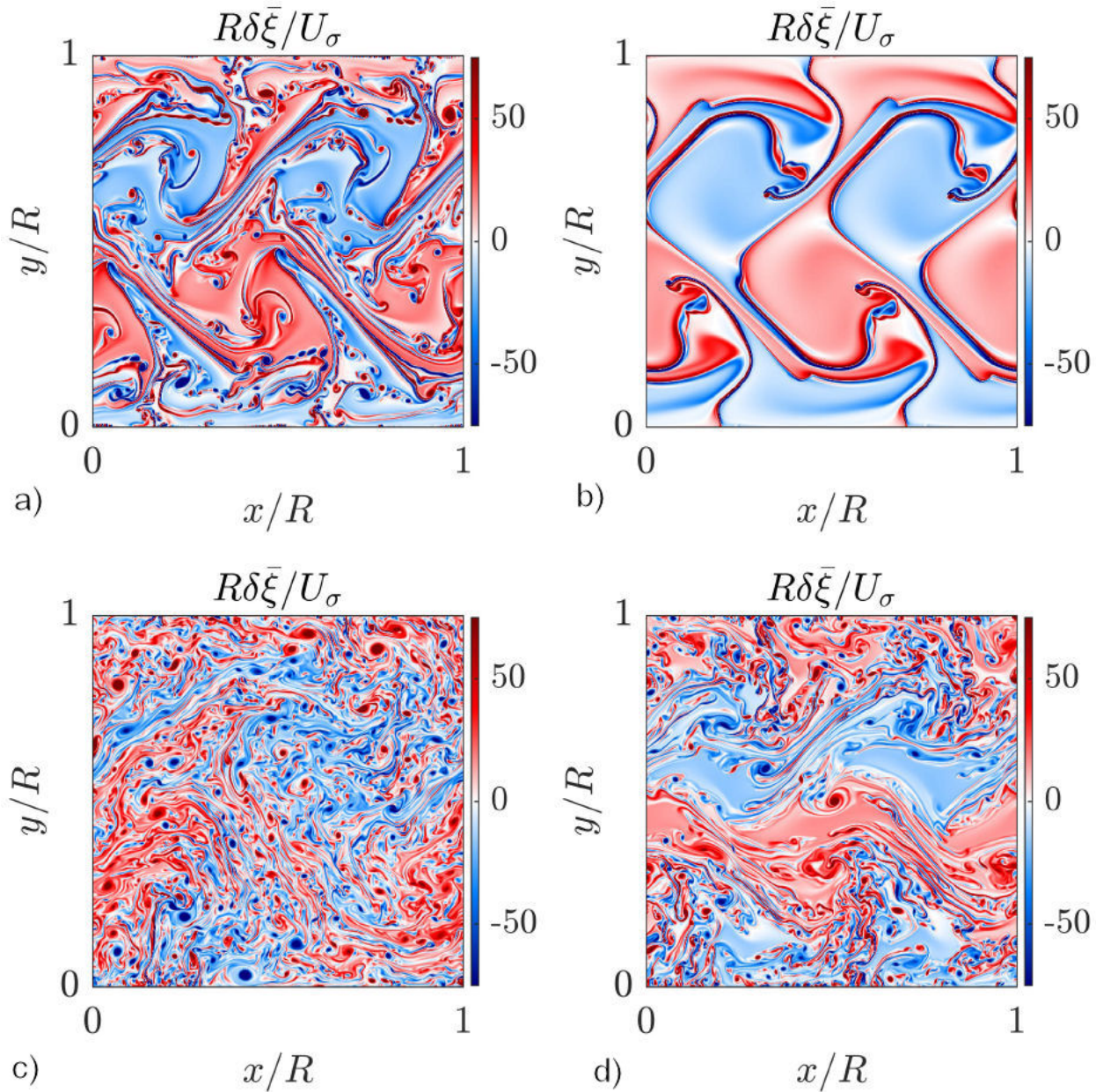
FIGURE 7. a) Snapshots at $U_\sigma t/R = 2$ (top) and 3 (bottom) of the nonlinear evolution of the potential vorticity perturbation to spectrally unstable basic state potential vorticity (58d) with $\alpha = 3$, $\mu = 0$, $b = 0$, and $S = 0$. a), c) As in the left column, but based on the IL^0QG, for which $S = 0$ and $\mu = 0$ (the buoyancy field is vertically uniform in this model).

initialized from the same basic state as the $\text{IL}^{(0,1)}\text{QG}$ except that in the IL^0QG, $\psi_{\sigma^2} = 0$, *i.e.*, the buoyancy is vertically uniform, so $S = 0$ and $\mu = 0$. For the parameters chosen and wavenumber-(2,1), the growth rate of the initial perturbation in the IL^0QG coincides with that in the $\text{IL}^{(0,1)}\text{QG}$. Comparing the left and right columns of Fig. 7, it is clear that submesoscale wave activity in the $\text{IL}^{(0,1)}\text{QG}$ can be more intense than, or at least as intense as, in the IL^0QG.

7. Concluding remarks

In this paper, we have investigated the properties of a thermal rotating shallow-water model with uniform stratification for subinertial upper-ocean dynamics, and carried out a stability analysis in the model. The model has an active layer, limited above by a rigid interface with the atmosphere, which freely floats atop an infinitely deep inert (abyssal) layer. The dynamics in the model is quasigeostrophic (QG). Unlike the adiabatic reduced-gravity QG model, the thermal model allows buoyancy (temperature) to vary laterally (*i.e.*, in the horizontal) and time. This enables the incorporation of heat and freshwater fluxes across the ocean surface. By con-

trast with the standard thermal model, the model considered here includes uniform stratification, still maintaining the two-dimensional structure of the thermal and adiabatic (*i.e.*, with a homogeneous density) models. The model is a special case of a recently derived extended theory of thermal models with geometry [6]. The QG version of the extended family of models is referred to as $IL^{(0,n)}QG$. Here IL stands for inhomogeneous layer. The first slot in the superscript of IL refers to the amount of vertical variation of the horizontal velocity with depth and the second one to the (whole) degree of a polynomial expansion of the buoyancy in the vertical coordinate. The particular stratified thermal QG model considered here is the $IL^{(0,1)}QG$ member of that family. The standard thermal QG model [20, 49, 55] is referred to as the IL^0QG, while the adiabatic QG model [41] to as the HLQG.

7.1. Main findings

The $IL^{(0,1)}QG$ has unique solutions, it possess a Kelvin–Noether-like circulation theorem along material loops stating that creation (or annihilation) of circulation is due to the misalignment between the gradients of layer thickness and buoyancy, and is manifestly Hamiltonian with a Lie–Poisson bracket. Geometrically, the bracket is a product for a realization Lie enveloping algebra on functionals in the dual of the Lie algebra of the Lie group obtained by extending the group of symplectic diffeomorphisms of the fluid domain, chosen here to be a periodic zonal channel of the β-plane, by semidirect product with two copies of the space of smooth functions on that domain. The induced algebra representation on the space of functions is given by the canonical Poisson bracket in $\mathbb{R}^2$. This Hamiltonian structure is not spoiled by the addition of certain type of topographic forcing. The $IL^{(0,1)}QG$ thus preserves energy and zonal momentum, respectively related to symmetry under time shits and zonal translations by Noether's theorem. In addition to these conservation laws, the model has integrals of motion that form the kernel of the Lie–Poisson bracket, known as Casimirs. Unlike the usual situation in Lie–Poisson Hamiltonian systems, the $IL^{(0,1)}QG$ also supports a class of motion integrals which neither form the kernel of the bracket nor are related to any explicit symmetries of the system via Noether's theorem. To the best of our knowledge, such integrals have so far never been reported. The model sustains the usual Rossby waves and a neutral model, both riding on a reference state, *i.e.*, one with no currents, a special type of it being the vacuum state, *i.e.*, one with vanishing energy. Positive definiteness of a general integral of motion, called a free energy, quadratic on the deviation from the reference state prevents perturbations of arbitrary shape and size on such a state from spuriously growing. An exception is the vacuum state, as perturbations on this state have positive-semidefinite free energy associate. Spurious growth of such perturbations cannot be prevented using free energy conservation.

The stability analysis carried out in the $IL^{(0,1)}QG$ was applied on a family of basic states representing baroclinic zonal jets with curvature in the velocity vertical profile. The $IL^{(0,1)}QG$ has velocity independent of depth. However, by the thermal-wind balance the velocity is implicitly vertically sheared. We found that a current in this family is spectrally stable, *i.e.*, with respect to infinitesimally small normal-mode perturbations, when the gradients of vertically averaged (mean) and layer thickness have like signs and the ratio of mean buoyancy and buoyancy frequency gradients are larger than a fraction of the reference layer thickness and vice versa. In the limit of very weak stratification, the growth rate of long perturbations, *i.e.*, with wavelengths of the order of the equivalent barotropic Rossby deformation radius, are found to saturate. By contrast, perturbations with wavelengths of the order of the gravest Rossby radius have vanishing growth rate. Only a subset of the spectrally stable states was possible to be shown stable with respect to finite-size perturbations of arbitrary structure using the integrals of motion by means of the application of Arnold's method. These integrals exclude the weak Casimir integrals, which form the kernel of the Lie-Poisson bracket for the potential vorticity evolution independent of the details of the buoyancy as this is advected under the flow. The role of these integrals in constraining stratified thermal flow remains to be understood. The states shown stable using Arnold's method are of Lyapunov type, *i.e.*, the instantaneous perturbation distance to such states as measured using an L^2 norm is bounded at all times by a multiple of the initial distance to them. These Lyapunov-stable states were used to *a priori* bound the nonlinear growth of perturbations to spectrally unstable states, thereby preventing evolution in the $IL^{(0,1)}QG$ from undergoing an ultraviolet explosion. This is extensible to perturbations to any unstable state, including the vacuum state, whose free energy can be vanishing.

Our findings do not support the generality of earlier numerical evidence suggesting that suppression of sub-deformation scale (*i.e.*, submesoscale) wave activity is a result of the inclusion of stratification in thermal shallow-water theory. We backed up the latter with results of direct, fully nonlinear simulations of the $IL^{(0,1)}QG$ and IL^0QG, which did not include topographic forcing as previously considered.

7.2. Outlook

Left for future investigation is uncovering the origins of the non-Casimir integrals of motion in the $IL^{(0,1)}QG$ model. Preliminary investigations utilizing the primitive-equation parent model [6] suggest that these conservation laws are linked through Noether's theorem, akin to Casimirs, to the invariance of Eulerian variables under particle relabeling. Also slated for future exploration is the integration of structure-preserving algorithms to provide a more precise framing of the fully nonlinear evolution in the $IL^{(0,1)}QG$ model compared to the IL^0QG model. This endeavor should be approached in tandem with understanding turbulence dynamics in these models, which deviate from those in HLQG due to the absence of enstrophy conservation, and its implica-

tions for observations. One notable challenge is devising a geometric (Lie–Poisson) integrator for flows on the annulus, as current methods are limited to the torus or the sphere *e.g.*, [12, 37].

Glossary of fundamental geophysical fluid concepts

Coriolis force. The only "fictitious" force required to make the fluid motion equations valid in a frame rotating with the Earth when the centrifugal force in that frame is balanced out by the gravitational force on a horizontal plane.

Coriolis parameter. Twice the Earth's local vertical angular velocity.

Boussinesq approximation. An approximation where density variations are ignored except where they appear multiplied by the acceleration due to gravity, that is, the vector composition of the gravitational and centrifugal accelerations.

Primitive equations. Three-dimensional Euler equations for arbitrary stratified incompressible fluid with Coriolis force in the horizontal and the hydrostatic and Boussinesq approximations.

Rossby number. A dimensionless number defined as the ratio of inertial to Coriolis acceleration.

Quasigeostrophic equations. Leading-order approximation to the primitive equations in the asymptotic limit of small Rossby number.

Thermal-wind balance. A balance between the vertical derivative of the Coriolis force and the horizontal buoyancy gradient.

Baroclinic instability. Instability resulting when a current is perturbed off from thermal-wind balance.

Reduced gravity. An approximation suitable for describing upper-ocean variability, where an active fluid layer is bounded above by a rigid interface with the atmosphere and floats freely above a motionless, infinitely deep fluid.

Appendix

A. Numerical details of the direct simulations

The numerical simulation of the $\mathrm{IL}^{(0,1)}\mathrm{QG}$ employed a pseudosepectral scheme with fast Fourier transform (FFT) in x and discrete sine transform (DST) in y to invert (4d), but as written for the *perturbation* to the (unstable) basic state. We consistently wrote the entire set (4) accordingly. The DST imposes a homogeneous Dirichlet boundary condition on $\delta\bar{\psi}$ without spoiling the strict zero-normal-flow at the channel northern and southern walls boundary conditions, namely, $\partial_x\bar{\psi}|_{y=0,W} = 0$. A total of 512 grid points in each direction, zonal and meridional, was considered. Differentiation was done using dialiased FFT in each direction using the $3/2$ zero-padding rule (we tried Chebyshev differentiation in y, but this led to numerical instability). The equations were forward advanced using a fourth-order Runge–Kutta method with time step $\Delta t U_\sigma/R \approx 0.0001$ as resulting by applying the Courant–Friedrichs–Lewy condition. Finally, a small amount (roughly $-1.5 \times 10^{-11} U_\sigma R^3$) of biharmonic hyperviscosity was included to stabilize the time step. The same numerical treatment was applied to the simulation of the $\mathrm{IL}^0\mathrm{QG}$. Our confidence on the simulations is measured by how well the conservation laws in the $\mathrm{IL}^{(0,1)}\mathrm{QG}$ and $\mathrm{IL}^0\mathrm{QG}$ are represented. Take energy ($\mathcal{E}$), momentum ($\mathcal{M}$), and two Casimirs common to the $\mathrm{IL}^{(0,1)}\mathrm{QG}$ and $\mathrm{IL}^0\mathrm{QG}$, *e.g.*, $\mathcal{C}_{1,0}$ and $\mathcal{C}_{1,\cos\psi_\sigma}$; cf. (41) and (45). The absolute magnitude of the relative error with respect to the values of these quantities initially are about 19.2, 2.6, 2.8, and 2.9% for the $\mathrm{IL}^{(0,1)}\mathrm{QG}$, and 17.3, 12.2, 3.0, and 3.3% for the $\mathrm{IL}^0\mathrm{QG}$

Acknowledgments

---

i. On the occasion of the 50th anniversary of Departamento de Oceanografía Física of CICESE (Ensenada, Baja California, Mexico), we dedicate this paper to the memory of Pedro Ripa (1946–2001), who inspired us to follow him in listening to the whispers in the woods.

ii. In Ref. [6], $2g_\mathrm{r}$ is incorrectly referred to as the reference buoyancy jump at the bottom of the active layer.

1. Fernando Andrade-Canto, Francisco J. Beron-Vera, Gustavo J. Goni, Daniel Karrasch, Maria J. Olascoaga, and Joquin Trinanes. Carriers of *Sargassum* and mechanism for coastal inundation in the Caribbean Sea. *Phys. Fluids*, **34** (2022) 016602

2. Vladimir I. Arnold. *Vladimir I. Arnold - Collected Works: Hydrodynamics, Bifurcation Theory, and Algebraic Geometry 1965-1972*. Springer Berlin Heidelberg, (2014)

3. E. Beier. A numerical investigation of the annual variability in the Gulf of California. *J. Phys. Oceanogr.*, **27** (1997) 615

4. T.B. Benjamin. Impulse, flow force and variational principles. *IMA J. Appl. Math.*, **32** (1984) 3.

5. G. Boccaletti, R. Ferrari, and B. Fox-Kemper. Mixed layer instabilities and restratification. *J. Phys. Oceanogr.*, **37** (2007) 2228

6. F. J. Beron-Vera. Extended shallow-water theories with thermodynamics and geometry. *Phys. Fluids*, **33** (2021) 106605,

7. F. J. Beron-Vera. Multilayer shallow-water model with stratification and shear. *Rev. Mex. Fis.*, **67** (2021) 351.

8. F. J. Beron-Vera. Nonlinear saturation of thermal instabilities. *Phys. Fluids*, **33** (2021) 036608,

9. F. J. Beron-Vera and Erwin Luesink. Dual Euler–Poincaré/Lie–Poisson formulation of subinertial stratified thermal ocean flow with identification of Casimirs as Noether quantities (2025). https://doi.org/10.48550/arXiv.2412.05441.

10. D. Crisan, D. D. Holm, E. Luesink, P. R. Mensah, and W. Pan. Theoretical and computational analysis of the thermal quasigeostrophic model. *Journal of Nonlinear Science*, **33** (2023) 96,

11. Yangyang Cao, Alexander Kurganov, Yongle Liu, and Vladimir Zeitlin. Flux globalization based well-balanced path-conservative central-upwind scheme for two-layer thermal rotating shallow water equations. *Journal of Computational Physics*, **474** (2023) 111790,

12. Paolo Cifani, Milo Viviani, Erwin Luesink, Klas Modin, and Bernard J. Geurts. Casimir preserving spectrum of two-dimensional turbulence. *Phys. Rev. Fluids*, **7** (2022) L082601,

13. P. J. Dellar. Common Hamiltonian structure of the shallow water equations with horizontal temperature gradients and magnetic fields. *Phys. Fluids*, **15** (2003) 292

14. Christopher Eldred, Thomas Dubos, and Evaggelos Kritsikis. A quasi-Hamiltonian discretization of the thermal shallow water equations. *Journal of Computational Physics*, **379** (2019) 1

15. R. Fjørtoft. Application of integral theorems in deriving criteria of stability for laminar flows and for the baroclinic circular vortex. *Geofys. Publ.*, **17** (1950) 1

16. Y. Fukamachi, J. P. McCreary, and J. A. Proehl. Instability of density fronts in layer and continuously stratified models. *J. Geophys. Res.*, **100** (1995) 2559.

17. E. Gouzien, N. Lahaye, V. Zeitlin, and T. Dubos. Thermal instability in rotating shallow water with horizontal temperature/density gradients. *Physics of Fluids*, **29** (2017) 101702,

18. Darryl D. Holm, Ruiao Hu, and Oliver D. Street. *Coupling of Waves to Sea Surface Currents Via Horizontal Density Gradients*, page 109-133. (Springer International Publishing, 2022).

19. D. D. Holm and E. Luesink. Stochastic wave–current interaction in thermal shallow water dynamics. *J. Nonlinear Sci.*, **31** (2021) 29.

20. Darryl D. Holm, Erwin Luesink, and Wei Pan. Stochastic mesoscale circulation dynamics in the thermal ocean. *Phys. Fluids*, **33** (2021) 046603

21. D. D. Holm, J. E. Marsden, and T. S. Ratiu. The Euler-Poincaré equations in geophysical fluid dynamics. In J. Norbury and I. Roulstone, editors, *Large-Scale Atmosphere-Ocean Dynamics II: Geometric Methods and Models*, pages 251-299. (Cambridge University, 2002).

22. D. D. Holm, J. E. Marsden, T. Ratiu, and A. Weinstein. Nonlinear stability of fluid and plasma equilibria. *Phys. Rep.*, **123** (1985) 1,

23. Darryl D. Holm. Ideal shallow water dynamics in a rotating frame. MPE CDT PDE Lecture Notes, (2015)

24. Alexander Kurganov, Yongle Liu, and Vladimir Zeitlin. Moist-convective thermal rotating shallow water model. *Physics of Fluids*, **32** (2020) 066601,

25. M. D. Kruskal and C. Oberman. Stability of plasma in static equilibrium. *Phys. Fluids*, **1** (1958) 275,

26. Noé Lahaye, Olivier Larroque, and Vladimir Zeitlin. Equatorial modons in thermal rotating shallow water model. *Journal of Fluid Mechanics*, **984** (2024)

27. D. Lewis, J. Marsden, and R. Montgomery. The Hamiltonian structure for dynamic free boundary problem. *Physica D*, **18** (1986) 391.

28. Noe Lahaye, Vladimir Zeitlin, and Thomas Dubos. Coherent dipoles in a mixed layer with variable buoyancy: Theory compared to observations. *Ocean Modelling*, **153** (2020) 101673.

29. A. Mahadevan. The impact of submesoscale physics on primary productivity of plankton. *Annu. Rev. Mar. Sci.*, **8** (2016) 161

30. Dennis J. McGillicuddy. Mechanisms of physical-biological-biogeochemical interaction at the oceanic mesoscale. *Annual Review of Marine Science*, **8** (2016) 125

31. J. C. McWilliams. Submesoscale currents in the ocean. *Proc R Soc A*, **472** (2016) 20160117

32. P. J. Morrison and S. Eliezer. Spontaneous symmetry breaking and neutral stability in the noncanonical hamiltonian formalism. *Physical Review A*, **33** (1986) 4205

33. P. J. Morrison and J. M. Greene. Noncanonical Hamiltonian density formulation of hydrodynamics and ideal magnetohydrodynamics. *Phys. Rev. Lett.*, **45** (1980) 790

34. P. J. Morrison and R. D. Hazeltine. Hamiltonian formulation of reduced magnetohydrodynamics. *Phys. Fluids*, **27** (1984) 886

35. J. P. McCreary and P.K. Kundu. A numerical investigation of the Somali current during the southwest monsoon. *J. Mar. Res.*, **46** (1988) 25.

36. P. J. Morrison. Hamiltonian description of the ideal fluid. *Rev. Mod. Phys.*, **70** (1998) 467.

37. Klas Modin and Milo Viviani. A Casimir preserving scheme for long-time simulation of spherical ideal hydrodynamics. *Journal of Fluid Mechanics*, **884** (2019) A22.

38. J. J. O'Brien and R. O. Reid. The non-linear response of a two-layer, baroclinic ocean to a stationary, axially-symmetric hurricane: Part I: Upwelling induced by momentum transfer. *J. Atmos. Sci.*, **24** (1967) 197.

39. J. L. Ochoa, J. Sheinbaum, and E. G. Pavía. Inhomogeneous rodons. *J. Geophys. Res.*, **103** (1998) 24869.

40. J. Pedlosky. Finite-amplitude baroclinic waves at minimum critical shear. *J. Atmos. Sci.*, **39** (1982) 555.

41. J. Pedlosky. *Geophysical Fluid Dynamics*. (Springer, 2nd edition, 1987).

42. R. Pinet and E. Pavía. Stability of elliptical horizontally inhomogeneous rodons. *J. Fluid Mech.*, **416** (2000) 29.

43. P. Ripa. General stability conditions for zonal flows in a one-layer model on the beta-plane or the sphere. *J. Fluid Mech.*, **126** (1983) 463.

44. P. Ripa. Sistemas Hamiltonianos singulares. I: Planteamiento del caso discreto, Teorema de Noether. *Rev. Mex. Fís.*, **38** (1992) 984.

45. P. Ripa. Arnol'd's second stability theorem for the equivalent barotropic model. *J. Fluid Mech.*, **257** (1993) 597.

46. P. Ripa. Conservation laws for primitive equations models with inhomogeneous layers. *Geophys. Astrophys. Fluid Dyn.*, **70** (1993) 85.

47. P. Ripa. On improving a one-layer ocean model with thermodynamics. *J. Fluid Mech.*, **303** (1995) 169.

48. P. Ripa. Linear waves in a one-layer ocean model with thermodynamics. *J. Geophys. Res. C*, **101** (1996) 1233.

49. P. Ripa. Low frequency approximation of a vertically integrated ocean model with thermodynamics. *Rev. Mex. Fis.*, **42** (1996) 117.

50. P. Ripa. On the validity of layered models of ocean dynamics and thermodynamics with reduced vertical resolution. *Dyn. Atmos. Oceans*, **29** (1999) 1.

51. P. Ripa. Estabilidad e inestabilidad. Parte i: Uso de integrales de movimiento en el problema de estabilidad. *Rev. Mex. Fís.*, **42** (2000) 413.

52. P.S. Schopf and M.A. Cane. On equatorial dynamics, mixed layer physics and sea surface temperature. *J. Phys. Oceanogr.*, **13** (1983) 917.

53. T.G. Shepherd. Rigorous bounds on the nonlinear saturation of instabilities to parallel shear flows. *J. Fluid Mech.*, **196** (1988) 291.

54. T. G. Shepherd. Symmetries, conservation laws and Hamiltonian structure in geophysical fluid dynamics. *Adv. Geophys.*, **32** (1990) 287.

55. E. S. Warneford and P. J. Dellar. The quasi-geostrophic theory of the thermal shallow water equations. *J. Fluid Mech.*, **723** (2013) 374.

56. Emma S. Warneford and Paul J. Dellar. Thermal shallow water models of geostrophic turbulence in Jovian atmospheres. *Physics of Fluids*, **26** (2014) 016603.